TORQUE RIPPLE REDUCTION IN DIRECT TORQUE CONTROLLED INDUCTION MOTOR DRIVE BY USING FUZZY CONTROLLER

A THESIS SUBMITTED IN PARTIAL FULFILLMENT OF THE

REQUIREMENTS FOR THE DEGREE OF

MASTER OF TECHNOLOGY

IN

POWER CONTROL AND DRIVES

By

G. Venkata RamaKrishna.

Department of Electrical Engineering

National Institute of Technology

Rourkela-769008

2007

TORQUE RIPPLE REDUCTION IN DIRECT TORQUE CONTROLLED INDUCTION MOTOR DRIVE BY USING FUZZY CONTROLLER

A THESIS SUBMITTED IN PARTIAL FULFILLMENT OF THE

REQUIREMENTS FOR THE DEGREE OF

MASTER OF TECHNOLOGY

IN

POWER CONTROL AND DRIVES

By

G.VENKATA RAMAKRISHNA

Under the Guidance of

Prof. A K PANDA

Department of Electrical Engineering

National Institute of Technology

Rourkela-769008

2007

National Institute of Technology

Rourkela

CERTIFICATE

This is to certify that the thesis entitled, **"Torque ripple reduction in Direct Torque controlled Induction Motor Drive by using Fuzzy Controller"** submitted by Mr **G.Venkata RamaKrishna** in partial fulfillment of the requirements for the award of MASTER of Technology Degree in **Electrical Engineering** with specialization in **"Power Control and Drives"** at the National Institute of Technology, Rourkela (Deemed University) is an authentic work carried out by him/her under my/our supervision and guidance.

To the best of my knowledge, the matter embodied in the thesis has not been submitted to any other University/ Institute for the award of any degree or diploma.

Date:

Prof A K Panda
Dept of Electrical Engineering.
National Institute of Technology
Rourkela - 769008

ACKNOWLEDGEMENT

I would like to thank my supervisor Prof. **Dr. A. K. Panda**, Department of Electrical Engineering for his valuable guidance and constant motivation and support during the course of my thesis work in the last one year. I am thankful to Prof. **Dr. P. K. Nanda,** Head of the Electrical Engineering department for his valuable suggestions and constant encouragement all through the thesis work. I am extremely thankful to Prof. **Dr. P. C. Panda,** department of Electrical Engineering, who indirectly involved in my thesis work by providing Power System Modeling lab.

I am thankful to Mr. **T. Purna Chandra Rao** for his valuable help as Power System modeling lab in charge. I will be failing in my duty if I do not mention the laboratory staff and administrative staff of this department for their timely help. I would like to thank all whose direct and indirect support helped me completing my thesis in time.

My parents and my brother Mr. **G. V. Subhash**, receive my deepest gratitude and love for their dedication and the many years of support that provided the foundation for this work.

G. Venkata. RamaKrishna

M.Tech (Power Control and Drives)

CONTENTS

ABSTRACT

Direct torque control (DTC) of an induction motor fed by a voltage source inverter is a simple scheme that does not need long computation time and can be implanted without mechanical speed sensors and is insensitive to parameter variations. In principle, the motor terminal voltages and currents are sampled and used to estimate the motor flux and torque. Based on estimates of the flux position and the instantaneous errors in torque and stator flux magnitude, a voltage vector is selected to restrict the torque and the flux errors within their respective torque and flux hysteresis bands.

In the conventional DTC, the selected voltage vector is applied for the whole switching period regardless of the magnitude of the torque error. This can result in high torque ripple. A better drive performance can be achieved by varying the duty ratio of the selected voltage vector during each switching period according to the magnitude of the torque error and position of the stator flux. A duty ratio control scheme for an inverter-fed induction machine using DTC method is presented in this thesis. The use of the duty ratio control resulted in improved steady state torque response, with less torque ripple than the conventional DTC. Fuzzy logic control was used to implement the duty ratio controller. The effectiveness of the duty ratio method was verified by simulation using **MATLAB/SIMULINK®.**

LIST OF FIGURES

LIST OF TABLES

Chapter 1

INTRODUCTION

Historical Review

Features of Direct Torque Control

Statement of Problem

Overview of Thesis

INTRODUCTION

1.1 .HISTORICAL REVIEW:

The history of electrical motors goes back as far as 1820, when Hans Christian Oersted discovered the magnetic effect of an electric current. One year later, Michael Faraday discovered the electromagnetic rotation and built the first primitive D.C. motor. Faraday went on to discover electromagnetic induction in 1831, but it was not until 1883 that Tesla invented the A.C asynchronous motor [2]. Currently, the main types of electric motors are still the same, DC, AC asynchronous and Synchronous, all based on Oersted. Faraday and Tesla's theories developed and discovered more than a hundred years ago.

Before the introduction of micro-controllers and high switching frequency semiconductor devices, variable speed actuators were dominated by DC motors. Today, using modern high switching frequency power converters controlled by micro-controllers, the frequency, phase and magnitude of the input to an AC motor can be changed and hence the motor’s speed and torque can be controlled. AC motors combined with their drives have replaced DC motors in industrial applications due to their lower cost, better reliability, lower weight, and reduced maintenance requirement. Squirrel cage Induction motors are more widely used than all the rest of the electric motors put together as they have all the advantages of AC motors and they are easy to build [2].

The main advantage is that induction motors do not require an electrical connection between stationary and rotating parts of the motor. Therefore, they do not need any mechanical commutator (brushes), leading to the fact that they are maintenance free motors. Induction motors also have low weight and inertia, high efficiency and a high overload capability. Therefore, they are cheaper and more robust, and less proves to any failure at high speeds. Furthermore, the motor can work in explosive environments because no sparks are produced. Taking into account all the advantages outlined above, induction motors must be considered the perfect electrical to mechanical energy converter. However, mechanical energy is more than often required at variable speeds, where the speed control system is not a trivial matter.

The only effective way of producing an infinitely variable induction motor speed drive is to supply the induction motor with three phase voltages of variable frequency and variable amplitude. A variable frequency is required because the rotor

speed depends on the speed of the rotating magnetic field provided by the stator. A variable voltage is required because the motor impedance reduces at low frequencies and consequently the current has to be limited by means of reducing the supply voltages [3] [4] [5]. Before the days of power electronics, a limited speed control of induction motor was achieved by switching the three-stator windings from delta connection to star connection, allowing the voltage at the motor windings to be reduced. Induction motors are also available with more than three stator windings to allow a change of the number of pole pairs. However, a motor with several windings is more expensive because more than three connections to the motor are needed and only certain discrete speeds are available.

Another alternative method of speed control can be realized by means of a wound rotor induction motor, where the rotor winding ends are brought out to slip rings. However, this method obviously removes most of the advantages of induction motors and it also introduces additional losses. By connecting resistors or reactance in series with the stator windings of the induction motors, poor performance is achieved.

With the enormous advances made in semiconductor technology during the last 20 years, the required conditions for developing a proper induction motor drive are present. These conditions can be divided mainly in two groups:

- The decreasing cost and improved performance in power electronic switching devices.[5]
- The possibility of implementing complex algorithms in the new microprocessors.

However, one precondition had to be made, which was the development of suitable methods to control the speed of induction motors, because in contrast to its mechanical simplicity their complexity regarding their mathematical structure (multivariable and non-linear) is not a trivial matter.

Historically, several general controllers have been developed:

1.1.1 .Scalar controllers:

Despite the fact that "Voltage-Frequency" (V/f) is the simplest controller, it is the most widespread, being in the majority of the industrial applications. It is known as a scalar control and acts by imposing a constant relation between voltage and frequency. The structure is very simple and it is normally used without speed feedback. However, this controller doesn’t achieve a good accuracy in both speed and torque responses, mainly due to the fact that the stator flux and the torque are not directly controlled. Even though, as long as the parameters are identified, the accuracy in the speed can be 2% (except in a very low speed), and the dynamic response can be approximately around 50ms [6].

1.1.2. Vector Controllers:

In these types of controllers, there are control loops for controlling both the torque and the flux [BOS 1]. The most widespread controllers of this type are the ones that use vector transform such as either Park or Ku [3]. Its accuracy can reach values such as 0.5% regarding the speed and 2% regarding the torque, even when at stand still. The main disadvantages are the huge computational capability required and the compulsory good identification of the motor parameters [7] [8] [9].

1.1.3. Field Acceleration method:

This method is based on maintaining the amplitude and the phase of the stator current constant, while avoiding electromagnetic transients. Therefore, the equations used can be simplified saving the vector transformation, which occurs in vector controllers. This technique has achieved some computational reduction, thus overcoming the main problem with vector controllers and allowing this method to become an important alternative to vector controllers [10] [11] [12].

Fig. 1.1 shows a block diagram of an AC motor drive system [4]. A single-phase or three-phase AC power supply and an AC/DC converter provide a DC input to an inverter. A micro-controller decides the switching states for the inverter to control the motor's torque or speed. A sensing unit feeds back terminal values such as motor speed, voltage and current to the micro-controller as needed for the closed-loop control of the motor. Controllers used in AC motor drives are generally referred to as vector or field-oriented controllers mentioned above.

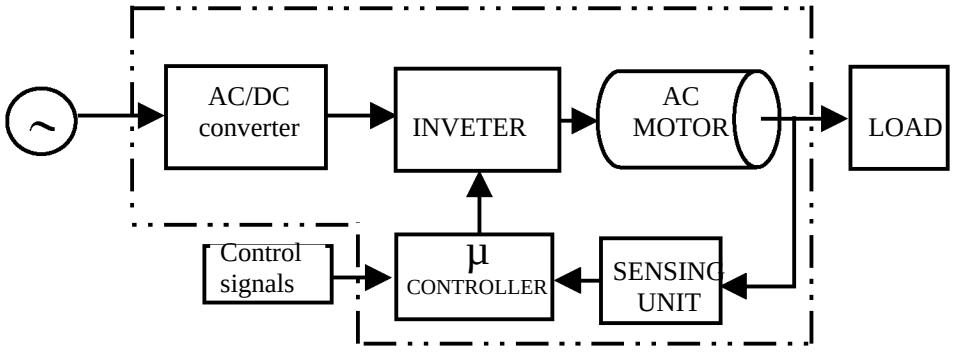

Fig 1.1.Block diagram for AC motor drive system

The field-oriented control methods are complex and sensitive to inaccuracy in the motor's parameter values. Therefore, in this field, a considerable research effort is devoted. The aim being to find even simpler methods of speed control for induction machines. One method, which is popular at the moment, is Direct Torque Control (DTC). This method has emerged

over the last decade to become one possible alternative to the well-known Vector Control of Induction Machines. Its main characteristic is the good performance, obtaining results as good as the classical vector control but with several advantages based on its simpler structure and control diagram.

1.1. FEATURES OF DIRECT TORQUE CONTROL :

DTC main features are as follows:

- Direct control of flux and torque.
- Indirect control of stator currents and voltages.
- Approximately sinusoidal stator fluxes and stator currents.
- High dynamic performance even at stand still.

The main advantages of DTC are:

- Absence of co-ordinate transforms.
- Absence of voltage modulator block, as well as other controllers such as PID for motor flux and torque.
- Minimal torque response time, even better than the vector controllers.

However, some disadvantages are also present such as:

- Possible problems during starting.
- Requirement of torque and flux estimators, implying the consequent parameters identification.
- Inherent torque and stator flux ripple.

1.3. STATEMENT OF THE PROBLEM:

A simplified variation of field orientation known as direct torque control (DTC) was developed by Takahashi [1] and Depenbrock [13]. Fig. 1.2 shows a DTC of an induction motor. In direct torque controlled induction motor drives, it is possible to control directly the stator flux linkage and the electromagnetic torque by the selection of an optimum inverter switching state. The selection of the switching state is made to restrict the flux and the torque errors within their respective hysteresis bands and to obtain the fastest torque response and highest efficiency at every instant. DTC is simpler than field-oriented control and less dependent on the motor model, since the stator resistance value is the only machine parameter used to estimate the stator flux.

One of the disadvantages of DTC is the high torque ripple. Under constant load in steady state, an active switching state causes the torque to continue to increase past its reference value until the end of the switching period. Then a zero voltage vector is applied for the next switching period causing the torque to continue to decrease below its reference value until the end of the switching period. That results in high torque

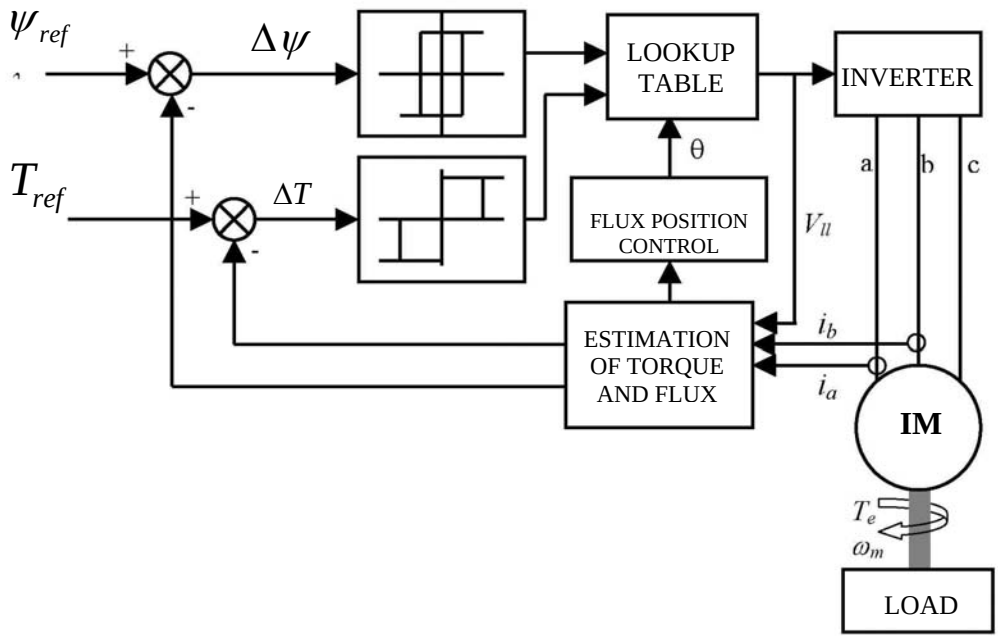

Fig 1.2.Direct torque control scheme

ripple as shown in Fig. 1.3(a). A possible solution to reduce the torque ripple is to use a high switching frequency; however, that requires expensive processors and switching devices. A less expensive solution is to use duty ratio control. In DTC with duty ratio control, the

selected voltage vector is applied for a part of the switching period rather than the complete switching period as in conventional DTC.

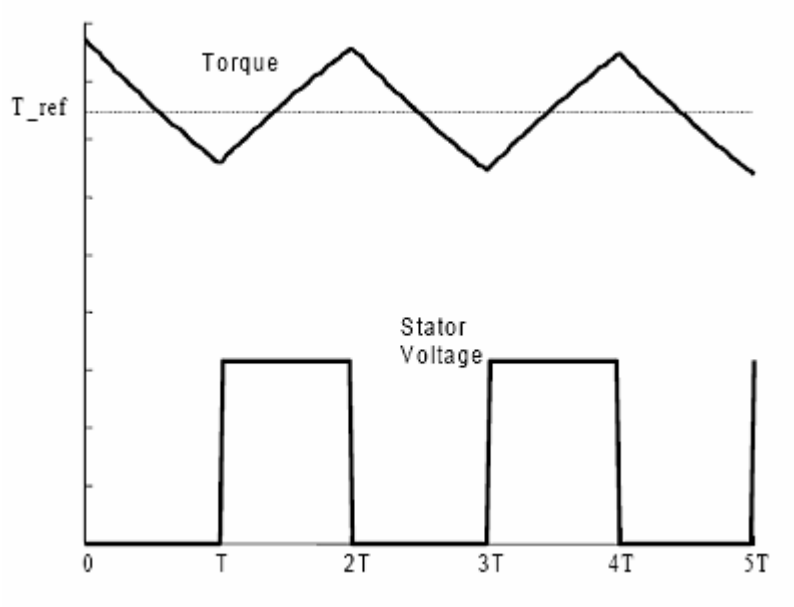

(a) Conventional DTC

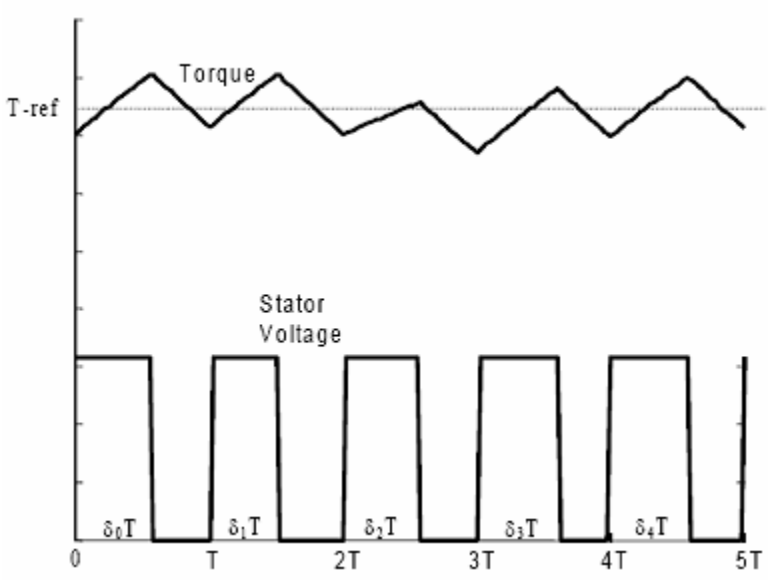

(b) DTC with duty ratio control

Fig 1.3 Effect of duty ratio control on torque ripple

By applying a nonzero voltage vector for only a portion of the switching period, and the zero voltage vector for the remainder of the period, the effective switching frequency is doubled. Therefore, over any single switching period, the torque variations above and below the average value are smaller, as shown `in Fig. 1.3(b). Further, because the duty ratio is controlled, the average stator voltage is adjusted directly. There is no need to make coarse corrections by the use of multiple switching periods with a nonzero voltage vector or a whole switching period with a zero voltage vector. The average phase voltage is adjusted more smoothly, and the overall torque ripple is reduced.

The use of a duty ratio fuzzy controller is proposed in [3][14]. The theme of this thesis is to verify by simulation that a DTC with a duty ratio fuzzy controller reduces the torque ripple compared to conventional DTC.

1.4. OVERVIEW OF THE THESIS:

Chapter II gives a review of the induction motor modeling, and of the field-oriented control methods and their limitations. A SIMULINK model is developed for the induction machine model and simulated for three phasors to two phase transformation of induction machine model.

Chapter III covers the fundamentals of the principle of DTC of induction motors and methods to deal with DTC limitations on flux estimation accuracy are discussed in detail. A SIMULINK model and MATLAB iterative technique programme are used to simulate the conventional DTC of induction motor.

Chapter IV details the theory and introduction of fuzzy logic controller used in the duty ratio controller used to minimize the torque ripple in DTC

Chapter V details the design of the duty ratio fuzzy controller used to minimize the torque ripple in DTC. The fuzzy logic controller determines the duty ratio according to torque and flux errors and flux position. SIMULINK/MATLAB is used to simulate this DTC with duty ratio fuzzy control.

Chapter VI covers the results and discussion on comparison of conventional DTC and fuzzy based DTC with duty ratio controller. The simulation results are presented and compared to the theoretical values.

Chapter VII gives the summary, conclusions and directions for future work.

Chapter 2

INDUCTION MOTOR MODEL AND GENERALITIES

Equations of the Induction Motor Model

Space phasor Notation

Torque Expressions

SIMULINK model

Interim Conclusions

INDUCTION MOTOR MODEL AND GENERALITIES

2.1 – EQUATIONS OF THE INDUCTION MACHINE MODEL:

2.1.1 – Introduction:

A dynamic model of the machine subjected to control must be known in order to understand and design vector controlled drives. Due to the fact that every good control has to face any possible change of the plant, it could be said that the dynamic model of the machine could be just a good approximation of the real plant. Nevertheless, the model should incorporate all the important dynamic effects occurring during both steady-state and transient operations. Furthermore, it should be valid for any changes in the inverter's supply such as voltages or currents [3] [4]. Such a model can be obtained by means of either the space vector phasor theory or two-axis theory of electrical machines. Despite the compactness and the simplicity of the space phasor theory, both methods are actually close and both methods will be explained.

For simplicity, the induction motor considered will have the following assumptions:

- Symmetrical two-pole, three phase windings.
- The slotting effects are neglected.
- The permeability of the iron parts is infinite.
- The flux density is radial in the air gap.
- Iron losses are neglected.
- The stator and the rotor windings are simplified as a single, multi-turn full pitch coil situated on the two sides of the air gap.

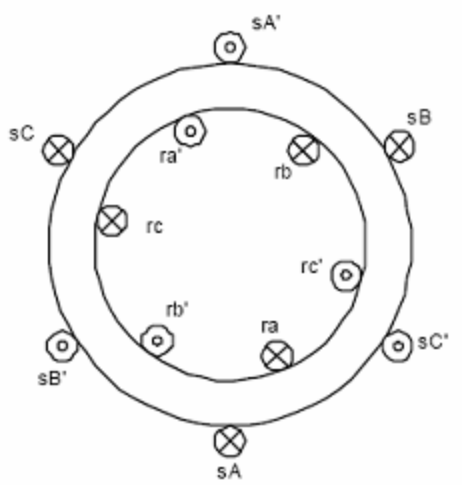

2.1. Cross section of elementary symmetrical three phase induction motor

2.1.2 – Voltage equations.

The stator voltages will be formulated in this section from the motor natural frame, which is the stationary reference frame fixed to the stator. In a similar way, the rotor voltages will be formulated to the rotating frame fixed to the rotor. In the stationary reference frame, the equations can be expressed as follows:

$$V_{sA} = R_s i_{sA}(t) + \frac{d\psi_{sA}(t)}{dt} \quad \text{---------- (2.1)}$$

$$V_{sB} = R_s i_{sB}(t) + \frac{d\psi_{sB}(t)}{dt} \quad \text{---------- (2.2)}$$

$$V_{sC} = R_s i_{sC}(t) + \frac{d\psi_{sC}(t)}{dt} \quad \text{---------- (2.3)}$$

Similar expressions can be obtained for the rotor:

$$V_{rA} = R_r i_{rA}(t) + \frac{d\psi_{rA}(t)}{dt} \quad \text{---------- (2.4)}$$

$$V_{rB} = R_r i_{rB}(t) + \frac{d\psi_{rB}(t)}{dt} \quad \text{---------- (2.5)}$$

$$V_{rC} = R_r i_{rC}(t) + \frac{d\psi_{rC}(t)}{dt} \quad \text{---------- (2.6)}$$

The instantaneous stator flux linkage values per phase can be expressed as:

$$\begin{aligned}
\psi_{sA} &= \overline{L_s} i_{sa} + \overline{M_s} i_{sB} + \overline{M_s} i_{sC} + \overline{M_{sr}} \cos\theta_m i_{ra} + \overline{M_{sr}} \cos(\theta_m + 2\pi/3) i_{rb} + \overline{M_{sr}} \cos(\theta_m + 4\pi/3) i_{rc} \\
\psi_{sA} &= \overline{M_s} i_{sa} + \overline{L_s} i_{sB} + \overline{M_s} i_{sC} + \overline{M_{sr}} \cos(\theta_m + 4\pi/3) i_{ra} + \overline{M_{sr}} \cos\theta_m i_{rb} + \overline{M_{sr}} \cos(\theta_m + 2\pi/3) i_{rc} \\
\psi_{sA} &= \overline{M_s} i_{sa} + \overline{M_s} i_{sB} + \overline{L_s} i_{sC} + \overline{M_{sr}} \cos(\theta_m + 2\pi/3) i_{ra} + \overline{M_{sr}} \cos(\theta_m + 4\pi/3) i_{rb} + \overline{M_{sr}} \cos\theta_m i_{rc}
\end{aligned} \quad \text{---------- (2.7)}$$

In a similar way, the rotor flux linkages can be expressed as follows:

$$\begin{aligned}
\psi_{ra} &= \overline{M_{sr}} \cos(-\theta_m) i_{sA} + \overline{M_{sr}} \cos(-\theta_m + 2\pi/3) i_{sB} + \overline{M_{sr}} \cos(-\theta_m + 4\pi/3) i_{sC} + \overline{L_r} i_{ra} + \overline{M_r} i_{rb} + \overline{M_r} i_{rc} \\
\psi_{rb} &= \overline{M_{sr}} \cos(-\theta_m + 4\pi/3) i_{sA} + \overline{M_{sr}} \cos(-\theta_m) i_{sB} + \overline{M_{sr}} \cos(-\theta_m + 2\pi/3) i_{sC} + \overline{M_r} i_{ra} + \overline{L_r} i_{rb} + \overline{M_r} i_{rc} \\
\psi_{rc} &= \overline{M_{sr}} \cos(-\theta_m + 2\pi/3) i_{sA} + \overline{M_{sr}} \cos(-\theta_m + 4\pi/3) i_{sB} + \overline{M_{sr}} \cos(-\theta_m) i_{sC} + \overline{M_r} i_{ra} + \overline{M_r} i_{rb} + \overline{L_r} i_{rc}
\end{aligned} \quad \text{---------- (2.8)}$$

Taking into account all the previous equations, and using the matrix notation in order to compact all the expressions, the following expression is obtained:

$$\begin{bmatrix} V_{sA} \\ V_{sB} \\ V_{sC} \\ V_{ra} \\ V_{rb} \\ V_{rc} \end{bmatrix} = \begin{bmatrix} R_s + p_{Ls} & pM_s & pM_s & pM_{sr}\cos\theta_m & pM_{sr}\cos\theta_{ml} & pM_{sr}\cos\theta_{ml} \\ pM_s & R_s + pL_s & pM_s & pM_{sr}\cos\theta_{ml} & pM_{sr}\cos\theta_m & pM_{sr}\cos\theta_{ml} \\ pM_s & pM_s & R_s + pL_s & pM_{sr}\cos\theta_{ml} & pM_{sr}\cos\theta_{ml} & pM_{sr}\cos\theta_m \\ pM_{sr}\cos\theta_m & pM_{sr}\cos\theta_{ml} & pM_{sr}\cos\theta_{ml} & R_r + pL_r & pM_r & pM_r \\ pM_{sr}\cos\theta_{ml} & pM_{sr}\cos\theta_m & pM_{sr}\cos\theta_{ml} & pM_r & R_r + pL_r & pM_r \\ pM_{sr}\cos\theta_m & pM_{sr}\cos\theta_{ml} & pM_{sr}\cos\theta_m & pM_r & pM_r & R_r + pL_r \end{bmatrix} \begin{bmatrix} i_{sA} \\ i_{sB} \\ i_{sC} \\ i_{ra} \\ i_{rb} \\ i_{rc} \end{bmatrix}$$

--------- (2.9)

2.1.3 – Applying Park's transform:

In order to reduce the expressions of the induction motor equation voltages given in equation 2.1 to equation 2.6 and obtain constant coefficients in the differential equations, the Park's transform will be applied. Physically, it can be understood as transforming the three windings of the induction motor to just two windings, as it is shown in figure 2.2 [3].

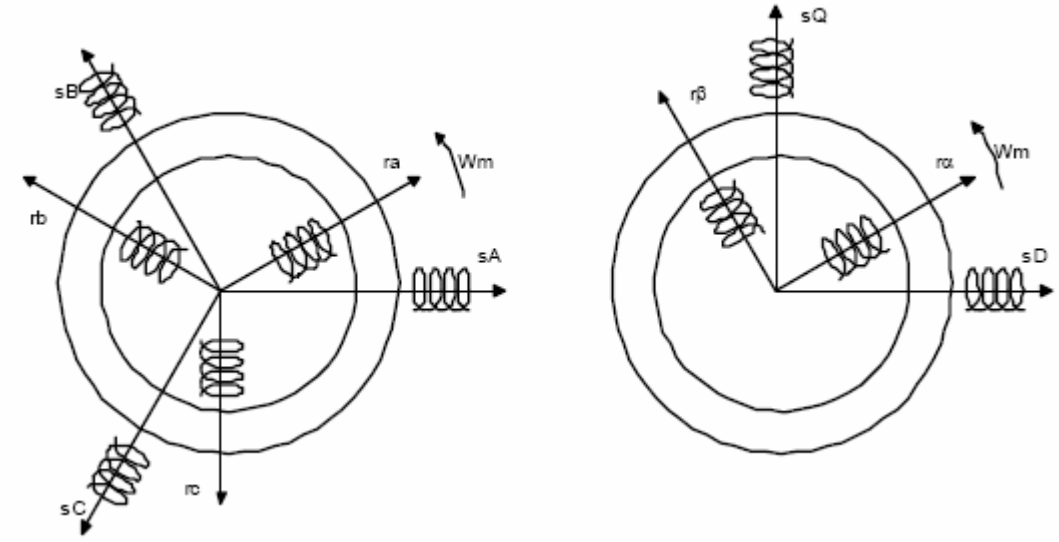

2.2. Scheme of equivalent axis transformation

In the symmetrical three-phase machine, the direct- and the quadrature-axis stator magnitudes are fictitious. The equivalencies for these direct (D) and quadrature (Q) magnitudes with the magnitudes per phase are as follows:

$$\begin{bmatrix} V_{sD} \\ V_{sQ} \\ V_{s0} \end{bmatrix} = c. \begin{bmatrix} \cos\theta & \cos(\theta - 2\pi/3) & \cos(\theta + 2\pi/3) \\ -\sin\theta & -\sin(\theta - 2\pi/3) & -\sin(\theta + 2\pi/3) \\ 1/\sqrt{2} & 1/\sqrt{2} & 1/\sqrt{2} \end{bmatrix} . \begin{bmatrix} V_{sA} \\ V_{sB} \\ V_{sC} \end{bmatrix}$$

---------- (2.10)

$$\begin{bmatrix} V_{sA} \\ V_{sB} \\ V_{sC} \end{bmatrix} = c. \begin{bmatrix} \cos\theta & -\sin\theta & 1/\sqrt{2} \\ \cos(\theta - 2\pi/3) & -\sin(\theta - 2\pi/3) & 1/\sqrt{2} \\ \cos(\theta + 2\pi/3) & -\sin(\theta + 2\pi/3) & 1/\sqrt{2} \end{bmatrix} . \begin{bmatrix} V_{sD} \\ V_{sQ} \\ V_{s0} \end{bmatrix} \quad \text{---------- (2.11)}$$

Where "c" is a constant that can take either the values 2/3 or 1 for the so-called non-power invariant form or the value $\sqrt{2/3}$ for the power-invariant form as it is explained in section 2.3.3. These previous equations can be applied as well for any other magnitudes such as currents and fluxes. Notice how the expression 2.9 can be simplified into a much smaller expression in 2.12 by means of applying the mentioned Park's transform.

$$\begin{bmatrix} V_{sD} \\ V_{sQ} \\ V_{r\alpha} \\ V_{r\beta} \end{bmatrix} = \begin{bmatrix} R_s + pL_s & -L_s p\theta_s & pL_m & -L_m(P.w_m + p\theta_r \\ L_s p\theta_s & R_s + pL_s & L_m(P.w_m + p\theta_r) & pL_m \\ pL_m & -L_m(p\theta_s - P.w_m) & R_r + pL_r & -L_r p\theta_r \\ L_m(p\theta_s - P.w_m) & pL_m & L_r p\theta_r & R_r + pL_r \end{bmatrix} . \begin{bmatrix} i_{sD} \\ i_{sQ} \\ i_{r\alpha} \\ i_{r\beta} \end{bmatrix}$$

--------- (2.12)

where L_S=L_S-L_m, L_r=L_r-L_m and $L_m = \frac{3}{2}\overline{M}_{sr}$. --------- (2.13)

2.1.4 – Voltage matrix equations:

If the matrix expression 2.12 is simplified, new matrixes are obtained as shown in equations

2.1.4.1 – Fixed to the stator.

It means that $w_s = 0$ and consequently $w_r = -w_m$.

$$\begin{bmatrix} V_{sD} \\ V_{sQ} \\ V_{rd} \\ V_{rq} \end{bmatrix} = \begin{bmatrix} R_s + pL_s & 0 & pL_m & 0 \\ 0 & R_s + pL_s & 0 & pL_m \\ pL_m & P.w_m L_m & R_r + pL_r & P.w_m L_r \\ -P.w_m L_m & pL_m & -P.w_m L_r & R_r + pL_r \end{bmatrix} . \begin{bmatrix} i_{sD} \\ i_{sQ} \\ i_{rd} \\ i_{rq} \end{bmatrix} \quad \text{---------- (2.14)}$$

2.1.4.2 – Fixed to the rotor.

It means that $w_r = 0$ and consequently $w_s = w_m$.

$$\begin{bmatrix} V_{sD} \\ V_{sQ} \\ V_{rd} \\ V_{rq} \end{bmatrix} = \begin{bmatrix} R_s + pL_s & -L_s P.w_m & pL_m & -L_m P.w_m \\ L_s P.w_m & R_s + pL_s & L_m P.w_m & pL_m \\ pL_m & 0 & R_r + pL_r & 0 \\ 0 & pL_m & 0 & R_r + pL_r \end{bmatrix} . \begin{bmatrix} i_{sD} \\ i_{sQ} \\ i_{rd} \\ i_{rq} \end{bmatrix} \qquad \text{--------- (2.15)}$$

2.1.4.3 – Fixed to the synchronism.

It means that $w_r = s.w_s$.

$$\begin{bmatrix} V_{sD} \\ V_{sQ} \\ V_{rd} \\ V_{rq} \end{bmatrix} = \begin{bmatrix} R_s + pL_s & -L_s w_s & pL_m & -L_m w_s \\ L_s w_s & R_s + pL_s & L_m P.w_s & pL_m \\ pL_m & -L_m s.w_s & R_r + pL_r & -L_r s w_s \\ L_m s.w_s & pL_m & L_r s w_s & R_r + pL_r \end{bmatrix} . \begin{bmatrix} i_{sD} \\ i_{sQ} \\ i_{rd} \\ i_{rq} \end{bmatrix} \qquad \text{--------- (2.16)}$$

2.2. SPACE PHASOR NOTATION:

2.2.1 – Introduction.

Space phasor notation allows the transformation of the natural instantaneous values of a three phase system onto a complex plane located in the cross section of the motor. In this plane, the space phasor rotate with an angular speed equal to the angular frequency of the three phase supply system. A space phasor rotating with the same angular speed, for example, can describe the rotating magnetic field. Moreover, in the special case of the steady state, where the supply voltage is sinusoidal and symmetric, the space phasor become equal to three-phase voltage phasors, allowing the analysis in terms of complex algebra. It is shown in figure 2.3 the equivalent schematic for this new model. In order to transform the induction motor model, in natural co-ordinates, into its equivalent space phasor form, the 120º operator is introduced:

$$a = e^{j2\pi/3}, a^2 = e^{j4\pi/3} \qquad \text{--------- (2.17)}$$

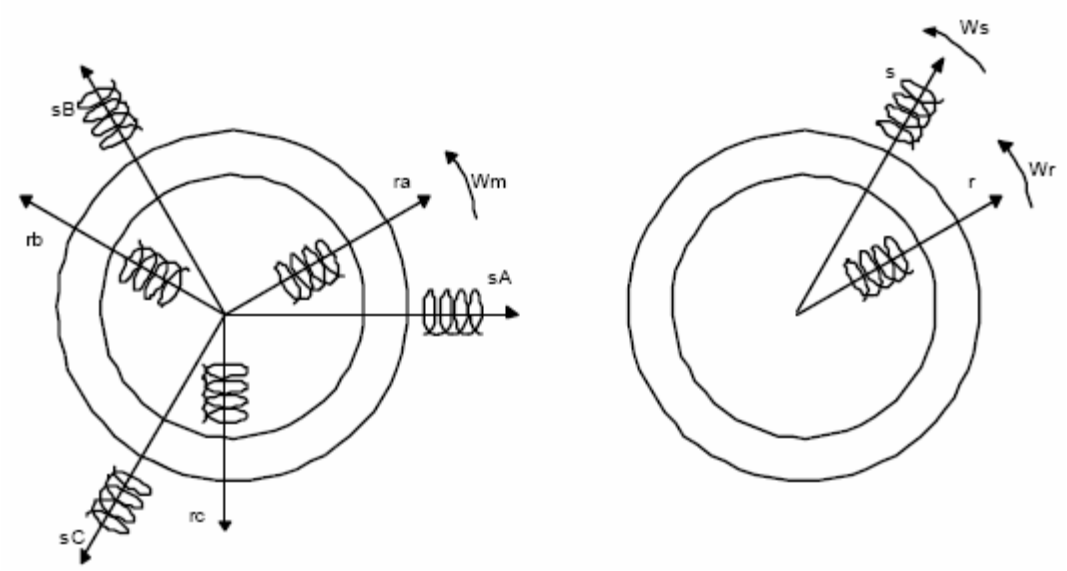

Fig 2.3 Space phasor representation of three phase quantities

Thus, the current stator space phasor can be expressed as follows:

$$\bar{i}_s = c.\left[1.i_{sA}(t) + a.i_{sB}(t) + a^2.i_{sC}(t)\right] \qquad \text{--------- (2.18)}$$

The factor "c", takes usually one of two different values either 2/3 or $\sqrt{2/3}$. The factor 2/3 makes the amplitude of any space phasor, which represents a three phase balanced system, equal to the amplitudes of one phase of the three-phase system. The factor $\sqrt{2/3}$ may also be

used to define the power invariance of a three-phase system with its equivalent two-phase system (see section 2.3.3).

2.2.2 – Current space phasors.

During this section the induction machine assumptions introduced in the section 2.1.1 will be further considered. It is represented in figure 2.4 the model of the induction machine with two different frames, the **D-Q** axis which represent the stationary frame fixed to the stator, and the **α-β** axis which represent rotating frame fixed to the rotor.

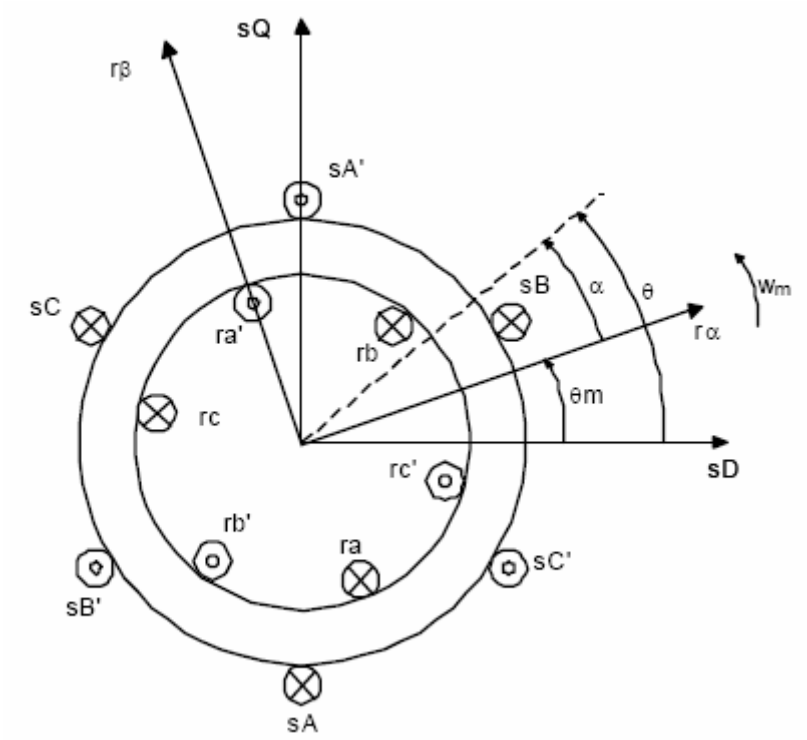

Fig 2.4.Cross-section of an elementary symmetrical three-phase machine, with two different frames, the D-Q axis which represent the stationary frame fixed to the stator, and α-β axis which represent rotating frame fixed to the rotor.

The stator current space phasor can be expressed as follows:

$$\bar{i}_s = \frac{2}{3}\left[i_{sA}(t) + a.i_{sB}(t) + a^2 i_{sC}(t) \right] = \left|\bar{i}_s\right| e^{j\theta} \qquad \text{--------- (2.19)}$$

Expressed in the reference frame fixed to the stator, the real-axis of this reference frame is denoted by **sD** and its imaginary-axis by **sQ**.

The equivalence between the stator phasor and the **D-Q** two-axis components is as follows:

$$\bar{i}_s = i_{sD}(t) + j.i_{sQ}(t) \qquad \text{-------- (2.20)}$$

Or:

$$\mathrm{Re}(\bar{i}_s) = \mathrm{Re}\left[\frac{2}{3}\left(i_{sA} + a.i_{sB} + a^2 i_{sC}\right)\right] = i_{sD} \quad \text{--------- (2.21)}$$

$$Im(\bar{i}_s) = \mathrm{Im}\left[\frac{2}{3}\left(i_{sA} + a.i_{sB} + a^2 i_{sC}\right)\right] = i_{sQ} \quad \text{--------- (2.22)}$$

The relationship between the space phasor current and the real stator phase currents can be expressed as follows:

$$\mathrm{Re}(\bar{i}_s) = \mathrm{Re}\left[\frac{2}{3}\left(i_{sA} + a.i_{sB} + a^2 i_{sC}\right)\right] = i_{sA} \quad \text{--------- (2.23)}$$

$$\mathrm{Re}(\bar{i}_s) = \mathrm{Re}\left[\frac{2}{3}\left(a^2.i_{sA} + i_{sB} + a.i_{sC}\right)\right] = i_{sB} \quad \text{--------- (2.24)}$$

$$\mathrm{Re}(\bar{i}_s) = \mathrm{Re}\left[\frac{2}{3}\left(a.i_{sA} + a^2.i_{sB} + i_{sC}\right)\right] = i_{sC} \quad \text{--------- (2.25)}$$

In a similar way, the space phasor of the rotor current can be written as follows:

$$\bar{i}_r = \frac{2}{3}\left[i_{ra}(t) + a.i_{rb}(t) + a^2 i_{rc}(t)\right] = \left|\bar{i}_r\right| e^{j\alpha} \quad \text{--------- (2.26)}$$

Expressed in the reference frame fixed to the rotor, the real-axis of this reference frame is denoted by rα and its imaginary-axis by rβ.

The space phasor of the rotor current expressed in the stationary reference frame fixed to the stator can be expressed as follows:

$$\bar{i}_r{}' = \left|\bar{i}_r\right| e^{j\theta} = \left|\bar{i}_r\right| e^{j(\alpha+\theta_m)} \quad \text{- -------- (2.27)}$$

The equivalence between the current rotor space phasor and the α-β two-axis is as follows:

$$\bar{i}_r = i_{r\alpha(t)} + j.i_{r\beta}(t) \quad \text{--------- (2.28)}$$

Or:

$$\mathrm{Re}(\bar{i}_r) = \mathrm{Re}\left[\frac{2}{3}\left(i_{ra} + a.i_{rb} + a^2 i_{rc}\right)\right] = i_{r\alpha} \quad \text{--------- (2.29)}$$

$$\mathrm{Im}(\bar{i}_r) = \mathrm{Im}\left[\frac{2}{3}\left(i_{ra} + a.i_{rb} + a^2 i_{rc}\right)\right] = i_{r\beta} \quad \text{--------- (2.30)}$$

The relationship between the space phasor current and the real stator currents can be expressed as follows:

$$\mathrm{Re}(\bar{i}_r) = \mathrm{Re}\left[\frac{2}{3}\left(i_{ra} + a.i_{rb} + a^2 i_{rc}\right)\right] = i_{ra} \quad \text{--------- (2.31)}$$

$$\mathrm{Re}(a^2\bar{i}_r) = \mathrm{Re}\left[\frac{2}{3}\left(a^2 i_{ra} + i_{rb} + a.i_{rc}\right)\right] = i_{rb} \quad \text{--------- (2.32)}$$

$$\mathrm{Re}(a\bar{i}_r) = \mathrm{Re}\left[\frac{2}{3}\left(a.i_{ra} + a^2.i_{rb} + i_{rc}\right)\right] = i_{rc} \quad \text{--------- (2.33)}$$

The magnetizing current space-phasor expressed in the stationary reference frame fixed to the stator can be obtained as follows:

$$\overline{i_m} = \overline{i_s} + \left(N_{re}/N_{se}\right)\overline{i_r'} \quad \text{--------- (2.34)}$$

2.2.3 Flux linkage space phasor:

In this section the flux linkages will be formulated in the stator phasor notation according to different reference frames.

2.2.3.1- Stator flux-linkage space phasor in the stationary reference frame fixed to the stator: Similarly to the definitions of the stator current and rotor current space phasors, it is possible to define a space phasor for the flux linkage as follows:

$$\overline{\psi_s} = \frac{2}{3}\left(\psi_{sA} + a\psi_{sB} + a^2\psi_{sC}\right) \quad \text{--------- (2.35)}$$

If the flux linkage equations 2.7 are substituted in equation 2.35, the space phasor for the stator flux linkage can be expressed as follows:

$$\overline{\psi_s} = \frac{2}{3}\begin{bmatrix} i_{sA}(L_s + aM_s + a^2M_s) + i_{sB}(M_s + aL_s + a^2M_s) + i_{sC}(M_s + aM_s + a^2L_s) + \\ +i_{ra}\left(M_{sr}\cos\theta_m + aM_{sr}\cos(\theta_m + 4\pi/3) + a^2M_{sr}\cos(\theta_m + 2\pi/3)\right) + \\ +i_{rb}\left(M_{sr}\cos(\theta_m + 2\pi/3) + aM_{sr}\cos\theta_m + a^2M_{sr}\cos(\theta_m + 4\pi/3)\right) + \\ +i_{rc}\left(M_{sr}\cos(\theta_m + 4\pi/3) + aM_{sr}\cos(\theta_m + 2\pi/3) + a^2M_{sr}\cos\theta_m\right) \end{bmatrix} \quad \text{--------- (2.36)}$$

Developing the previous expression 1.33, it is obtained the following expression:

$$\overline{\psi_s} = \frac{2}{3}\begin{bmatrix} i_{sA}(L_s + aM_s + a^2M_s) + ai_{sB}(a^2M_s + aL_s + aM_s) + a^2i_{sC}(M_s + aM_s + a^2L_s) + \\ +i_{ra}\left(M_{sr}\cos\theta_m + aM_{sr}\cos(\theta_m + 4\pi/3) + a^2M_{sr}\cos(\theta_m + 2\pi/3)\right) + \\ +a.i_{rb}\left(a^2M_{sr}\cos(\theta_m + 2\pi/3) + M_{sr}\cos\theta_m + aM_{sr}\cos(\theta_m + 4\pi/3)\right) + \\ +a^2.i_{rc}\left(aM_{sr}\cos(\theta_m + 4\pi/3) + a^2M_{sr}\cos(\theta_m + 2\pi/3) + M_{sr}\cos\theta_m\right) \end{bmatrix} \quad \text{------ (2.37)}$$

And finally, expression 2.37 can be represented as follows:

$$\begin{aligned}\overline{\psi_s} &= (L_s + aM_s + a^2M_s)i_s + \left(M_{sr}\cos\theta_m + aM_{sr}\cos(\theta_m + 4\pi/3) + a^2M_{sr}\cos(\theta_m + 2\pi/3)\right)\overline{i_r} \\ &= (L_s - M_s)\overline{i_s} + 1.5\overline{M_{sr}}\cos\theta_m.\overline{i_r} = (L_s - M_s)\overline{i_s} + 1.5\overline{M_{sr}}\,\overline{i_r}e^{j\theta_m} = (L_s - M_s)\overline{i_s} + 1.5\overline{M_{sr}}\,\overline{i_r'} \\ &= L_s\overline{i_s} + L_m\overline{i_r'}\end{aligned} \quad \text{--------- (2.38)}$$

Where Ls is the total three-phase stator inductance and Lm is the so-called three-phase magnetizing inductance. Finally, the space phasor of the flux linkage in the stator depends on two components, being the stator currents and the rotor currents.

Once more, the flux linkage magnitude can be expressed in two-axis as follows:

$$\overline{\psi_s} = \psi_{sD} + j\psi_{sQ} \quad \text{--------- (2.39)}$$

Where its direct component is equal to:

$$\psi_{sD} = L_s i_{sD} + L_m i_{rd} \quad \text{--------- (2.40)}$$

And its quadrature component is expressed as:

$$\psi_{sQ} = L_s i_{sQ} + L_m i_{rq} \quad \text{--------- (2.41)}$$

The relationship between the components i_{rd} and $i_{r\alpha}$ and i_{rq} and $i_{r\beta}$ may be introduced as follows:

$$\overline{i_r'} = i_{rd} + ji_{rq} = \overline{i_r}e^{j\theta_m} \quad \text{--------- (2.42)}$$

2.2.3.2- Rotor flux-linkage space phasor in the rotating reference frame fixed to the rotor:

The rotor flux linkage space phasor, fixed to the rotor natural frame can be defined as follows:

$$\overline{\psi_r} = \frac{2}{3}\left(\psi_{ra} + a\psi_{rb} + a^2\psi_{rc}\right) \quad \text{--------- (2.43)}$$

If the flux linkage equations 2.8 are substituted in equation 2.43, the space phasor for the rotor flux linkage can be expressed as follows:

$$\overline{\psi_r} = \frac{2}{3}\begin{bmatrix} i_{ra}(L_r + aM_r + a^2M_r) + i_{rb}(M_r + aL_r + a^2M_r) + i_{rc}(M_r + aM_r + a^2L_r) + \\ +i_{sA}\left(M_{sr}\cos\theta_m + aM_{sr}\cos(\theta_m + 2\pi/3) + a^2M_{sr}\cos(\theta_m + 4\pi/3)\right) + \\ +i_{sB}\left(M_{sr}\cos(\theta_m + 4\pi/3) + aM_{sr}\cos\theta_m + a^2M_{sr}\cos(\theta_m + 2\pi/3)\right) + \\ +i_{sC}\left(M_{sr}\cos(\theta_m + 2\pi/3) + aM_{sr}\cos(\theta_m + 4\pi/3) + a^2M_{sr}\cos\theta_m\right) \end{bmatrix} \text{----- (2.44)}$$

By re-arranging the previous expression 2.44, it can be expressed as:

$$\overline{\psi_r} = \frac{2}{3}\begin{bmatrix} i_{ra}(L_r + aM_r + a^2M_r) + ai_{rb}(a^2M_r + L_r + aM_s) + a^2i_{rc}(aM_r + a^2M_r + L_r) + \\ +i_{sA}\left(M_{sr}\cos\theta_m + aM_{sr}\cos(\theta_m + 2\pi/3) + a^2M_{sr}\cos(\theta_m + 4\pi/3)\right) + \\ +a.i_{sB}\left(a^2M_{sr}\cos(\theta_m + 4\pi/3) + M_{sr}\cos\theta_m + aM_{sr}\cos(\theta_m + 2\pi/3)\right) + \\ +a^2.i_{sC}\left(aM_{sr}\cos(\theta_m + 2\pi/3) + a^2M_{sr}\cos(\theta_m + 4\pi/3) + M_{sr}\cos\theta_m\right) \end{bmatrix} \text{--- (2.45)}$$

And finally

$$\begin{aligned} \overline{\psi_r} &= (L_r + aM_r + a^2M_r)\bar{i}_r + \left(M_{sr}\cos\theta_m + aM_{sr}\cos(\theta_m + 2\pi/3) + a^2M_{sr}\cos(\theta_m + 4\pi/3)\right)\bar{i}_s \\ &= (L_r - M_r)\bar{i}_r + 1.5\overline{M_{sr}}\cos(-\theta_m)\bar{i}_s = (L_r - M_r)\bar{i}_r + 1.5\overline{M_{sr}}\bar{i}_s e^{-j\theta_m} = (L_r - M_{sr})\bar{i}_r + 1.5\overline{M_{sr}}\bar{i}_s' \\ &= L_r\,\overline{i_r} + L_m\,\overline{i_s'} \end{aligned} \text{--------- (2.46)}$$

Where L_r is the total three-phase rotor inductance and Lm is the so-called three-phase magnetizing inductance. $\bar{i}_s'$ is the stator current space phasor expressed in the frame fixed to the rotor.

Once more the flux linkage magnitude can be expressed in the two-axis form as follows:

$$\overline{\psi}_r = \psi_{r\alpha} + j\psi_{r\beta} \text{--------- (2.47)}$$

Where its direct component is equal to:

$$\psi_{r\alpha} = L_r i_{r\alpha} + L_m i_{s\alpha} \text{--------- (2.48)}$$

And its quadrature component is expressed as:

$$\psi_{r\beta} = L_r i_{r\beta} + L_m i_{s\beta} \text{--------- (2.49)}$$

2.2.3.3- Rotor flux-linkage space phasor in the stationary reference frame fixed to the stator.

The rotor flux linkage can also be expressed in the stationary reference frame using the previously introduced transformation $e^{j\theta m}$, and can be written as:

$$\overline{\psi}_r' = \psi_{rd} + j\psi_{rq} = \overline{\psi}_r e^{j\theta_m} = \left(\psi_{r\alpha} + j\psi_{r\beta}\right)e^{j\theta_m} \text{--------- (2.50)}$$

The space phasor of the rotor flux linkage can be expressed according to the fixed coordinates as follows:

$$\overline{\psi}_r' = L_r\bar{i}_r' + L_m\bar{i}_s' e^{i\theta} = L_r\bar{i}_r' + L_m i_s \text{--------- (2.51)}$$

The relationship between the stator current referred to the stationary frame fixed to the stator and the rotational frame fixed to the rotor is as follows:

$$\bar{i}_s = \bar{i}'_s e^{j\theta_m}$$

$$\bar{i}_s e^{-j\theta_m} = \bar{i}'_s \qquad \text{--------- (2.52)}$$

Where

$$\bar{i}_s = i_{sD} + j i_{sQ}$$

$$\bar{i}'_s = i_{s\alpha} + j i_{s\beta} \qquad \text{--------- (2.53)}$$

From figure 1.5, the following equivalencies can be deduced:

$$\bar{i}_s = \left|\bar{i}_s\right| e^{j\theta}$$

$$\bar{i}'_s = \left|\bar{i}'_s\right| e^{i\alpha} = \left|\bar{i}'_s\right| e^{j(\theta-\theta_m)} = i_s e^{-j\theta_m} \qquad \text{--------- (2.54)}$$

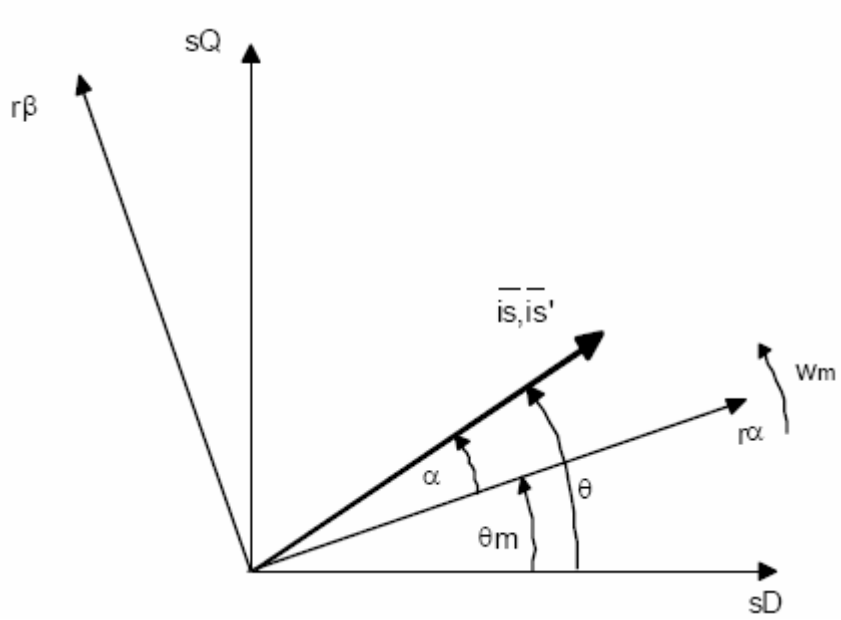

Fig 2.5.Stator-current space phasor expressed in accordance with the rotational frame fixed to the rotor and the stationary frame fixed to the stator.

2.2.3.4- Stator flux-linkage space phasor in the rotating reference frame fixed to the rotor:

Similarly than 2.2.3.3 section, it can be deduced the following expression:

$$\psi_s = \psi_s e^{-j\theta_m} = \left(L_s \bar{i}_s + L_m \bar{i}'_r\right) e^{-j\theta_m} = L_s \bar{i}'_s + L_m \bar{i}_r \qquad \text{--------- (2.55)}$$

2.2.4. – The space phasors of stator and rotor voltages.

The space phasors for the stator and rotor voltages can be defined in a similar way like the one used for other magnitudes.

$$\overline{V_s} = \frac{2}{3}\left[V_{sA}(t) + aV_{sB}(t) + a^2 V_{sC}(t)\right] = V_{sD} + jV_{sQ} = \frac{2}{3}\left(V_{sA} - \frac{1}{2}V_{sB} - \frac{1}{2}V_{sC}\right) + j\frac{1}{\sqrt{3}}\left(V_{sB} - V_{sC}\right) \text{---- (2.56)}$$

$$\overline{V_r} = \frac{2}{3}\left[V_{ra}(t) + aV_{rb}(t) + a^2 V_{rc}(t)\right] = V_{r\alpha} + jV_{r\beta} = \frac{2}{3}\left(V_{ra} - \frac{1}{2}V_{rb} - \frac{1}{2}V_{rc}\right) + j\frac{1}{\sqrt{3}}\left(V_{rb} - V_{rc}\right) \text{---- (2.57)}$$

Where the stator voltage space phasor is referred to the stator stationary frame and the rotor voltage space phasor is referred to the rotating frame fixed to the rotor. Provided the zero component is zero [3] [4], it can also be said that:

$$\begin{aligned} V_{sA} &= \mathrm{Re}(\overline{V}_s) \\ V_{sB} &= \mathrm{Re}(a^2 \overline{V}_s) \\ V_{sC} &= \mathrm{Re}(a \overline{V}_s) \end{aligned} \qquad \text{--------- (2.58)}$$

Equivalent expressions can also be obtained for the rotor.

2.3 TORQUE EXPRESSIONS:

2.3.1 - Introduction.

The general expression for the torque is as follows:

$$t_e = c\psi_s \times \bar{i}_r' \qquad \text{--------- (2.59)}$$

Where the "c" is a constant, ψ_s and $\bar{i}_r'$ are the space phasors of the stator flux and rotor current respectively, both referred to the stationary reference frame fixed to the stator.

The expression given above can also be expressed as follows:

$$t_e = c\,|\psi_s|.\left|\bar{i}_r\right|\sin\gamma \qquad \text{--------- (2.60)}$$

Where γ is the angle existing between the stator flux linkage and the rotor current. It follows that when $\gamma=90^o$ the torque obtained is the maximum and its expression is exactly equal to the one for the DC machines. Nevertheless, in DC machines the space distribution of both magnitudes is fixed in space, thus producing the maximum torque for all different magnitude values. Furthermore, both magnitudes can be controlled independently or separately. In an AC machine, however, it is much more difficult to realize this principle because both quantities are coupled and their position in space depends on both the stator and rotor positions. It is a further complication that in squirrel-cage machines, it is not possible to monitor the rotor current, unless the motor is specially prepared for this purpose in a special laboratory. It is impossible to find them in a real application. The search for a simple control scheme similar to the one for DC machines has led to the development of the so-called vector control schemes, where the point of obtaining two different currents, one for controlling the flux and the other one for the rotor current, is achieved [3] [4].

2.3.2 - Deduction of the torque expression by means of energy considerations.

Torque equation is being deduced by means of energy considerations. Therefore, the starting equation is as follows:

$$P_{mechanical} = P_{electric} - P_{loss} - P_{field}$$

Substituting the previous powers for its values, the equation can be expressed as follows:

$$t_e.w_r = \frac{3}{2}\left[\left(\mathrm{Re}(\bar{V}_s.\bar{i}_s^*) - R_s\left|i_s\right|^2 - \mathrm{Re}\left(\frac{d\psi_s}{dt}\bar{i}_s^*\right)\right) + \left(\mathrm{Re}(\bar{V}_r.\bar{i}_r^* - R_r\left|I_r'\right|^2 - \mathrm{Re}\left(\frac{d\psi'_r}{dt}I_r'^*\right)\right)\right] \text{--- (2.61)}$$

Since in the stationary reference frame, the stator voltage space phasor $\overline{V}_s$ can only be balanced by the stator ohmic drop, plus the rate of change of the stator flux linkage, the previous expression can be expressed as follows:

$$t_e.w_r = \frac{3}{2}\mathrm{Re}\left(-jw_r\overline{\psi_r}'\overline{i_r}'\right) = -\frac{3}{2}w_r\,\mathrm{Re}\left(j\overline{\psi_r}'\overline{i_r}'^{*}\right) = -\frac{3}{2}w_r\overline{\psi_r}' \times \overline{i_r}' \qquad \text{--------- (2.62)}$$

Expressing the equation in a general way for any number of pair of poles gives:

$$t_e = -\frac{3}{2}P\overline{\psi_r}' \times \overline{i_r}' \qquad \text{--------- (2.63)}$$

If equation 2.38 is substituted in equation 2.63 it is obtained the following expression for the torque:

$$t_e = \frac{3}{2}P\,\overline{\psi_s} \times \overline{i_s} \qquad \text{--------- (2.64)}$$

If the product is developed, expression 2,64 is as follows:

$$t_e = \frac{3}{2}P\left(\psi_{sD}.i_{sQ} - \psi_{sQ}.i_{sD}\right) \qquad \text{--------- (2.65)}$$

Finally, different expressions for the torque can be obtained as follows:

$$t_e = -\frac{3}{2}P\left(L_r\overline{i_r}' + L_m\overline{i_s}\right)\times\overline{i_r}' = -\frac{3}{2}PL_m\overline{I_s}\times\overline{i_r}' = -\frac{3}{2}PL_m\overline{I_s}'\times\overline{i_r} \qquad \text{--------- (2.66)}$$

$$t_e = -\frac{3}{2}P\frac{Lm}{Ls}\left(L_m\overline{i_r}' + L_s\overline{i_s}\right)\times\overline{i_r}' = -\frac{3Lm}{2Ls}P\overline{\psi_s}\times\overline{i_r}' = -\frac{3}{2}P\frac{L_m}{L_sL_r - L_m^{\,2}}\overline{\psi_s}\times\overline{\psi_r}'$$

2.3.3 – Torque constant.

The value of the torque constant can take two different values. These depend on the constant used in the space phasor. Both possibilities are shown in table 2.1..

Table 2.1 Torque constant values

	Non power invariant		*Power invariant*	
Torque constant	$3/2$		1	
Space phasor constant	*3→2*	*2→3*	*3→2*	*2→3*
	$2/3$	1	$\sqrt{2/3}$	$\sqrt{2/3}$

"3→2" means the change from three axis to either two axis or space phasor notation, and "2→3" either two axis or space phasor notation to three axis.

2.4 SIMULINK MODEL:

2.4.1 - Equations used in the model.

The final expressions used in the implemented models are obtained from all the previously introduced expressions. All equations have been re-arranged in order to use the operator 1/s instead of the operator p because the "Simulink" deals with the integrator better than with the derivation.

2.4.1.1 – Stator reference.

Stator and rotor fluxes can be expressed as follows:

$$\psi_{sD} = \frac{1}{s}\left(V_{sD} - R_s i_{sD}\right)$$

$$\psi_{sQ} = \frac{1}{s}\left(V_{sQ} - R_s i_{sQ}\right) \qquad \text{--------- (2.67)}$$

$$\psi'_{rd} = \frac{1}{s}\left(V_{rd}' - R_r I_{rd}' - P.w_m \psi_{rq}'\right) = \frac{1}{s}\left(-R_r i_{rd}' - P.w_m \psi_{rq}'\right)$$

$$\psi_{rq} = \frac{1}{s}\left(V_{rq}' - R_r i_{rq}' + P.w_m \psi_{rd}'\right) = \frac{1}{s}\left(-R_r i_{rq}' + P.w_m \psi_{rd}'\right)$$

Stator and rotor currents can be expressed as follows:

$$i_{sD} = \psi_{sD}\frac{L_r}{L_x} - \psi_{rd}'\frac{L_m}{L_x}$$

$$i_{sQ} = \psi_{sQ}\frac{L_r}{L_x} - \psi_{rq}'\frac{L_m}{L_x}$$

$$i_{rd} = \psi'_{rd}\frac{L_s}{L_x} - \psi_{sD}\frac{L_m}{L_x} \qquad \text{--------- (2.68)}$$

$$i_{rq} = \psi'_{rq}\frac{L_s}{L_x} - \psi_{sQ}\frac{L_m}{L_x}$$

Where $L_x = L_s L_r - L_m^{\,2}$

2.4.1.2 - Rotor reference.

Stator and rotor fluxes can be expressed as follows:

$$\psi_{rd} = \frac{1}{s}\left(V_{rd} - R_r i_{rd}\right) = 0 \qquad \text{--------- (2.69)}$$

$$\psi_{rq} = \frac{1}{s}\left(V_{rq} - R_r i_{rq}\right) = 0$$

$$\psi'_{sd} = \frac{1}{s}\left(V_{sd}' - R_s I_{sd}' + P.w_m \psi_{sq}'\right) = \frac{1}{s}\left(-R_r i_{rd}' - P.w_m \psi_{rq}'\right) \quad \text{--------- (2.70)}$$

$$\psi'_{sq} = \frac{1}{s}\left(V_{sq}' - R_r i_{sq}' - P.w_m \psi_{sd}'\right) = \frac{1}{s}\left(-R_r i_{rq}' + P.w_m \psi_{rd}'\right)$$

Stator and rotor currents can be expressed as follows:

$$i_{sD} = \psi'_{sD}\frac{L_r}{L_x} - \psi_{rd}'\frac{L_m}{L_x}$$

$$i_{sQ} = \psi'_{sQ}\frac{L_r}{L_x} - \psi_{rq}'\frac{L_m}{L_x}$$

$$i_{rd} = \psi_{rd}\frac{L_s}{L_x} - \psi'_{sD}\frac{L_m}{L_x} \quad \text{--------- (2.71)}$$

$$i_{rq} = \psi_{rq}\frac{L_s}{L_x} - \psi'_{sQ}\frac{L_m}{L_x}$$

Where $L_x = L_s L_r - L_m^{\,2}$

2.4.1.4 – Motion equation.

The motion equation is as follows:

$$t_e - t_L = J\frac{dw_m}{dt} + Dw_m \quad \text{--------- (2.72)}$$

Where, t_e is the electromagnetic torque, t_L is load torque, J is the inertia of the rotor, and finally the D is the damping constant.

Using the torque expressions 2.65, the previous motion equation can be expressed as follows:

$$P.c.\left(\psi_{sD}.i_{sQ} - \psi_{sQ}.i_{sD}\right) = t_L + w_m\left(D + Js\right)$$

$$w_r = \frac{P.c.\left(\psi_{sD}.i_{sQ} - \psi_{sQ}.i_{sD}\right) - t_L}{D + Js} \quad \text{--------- (2.73)}$$

Where P is the number of pair of poles and the torque constant take the values either 1 or 2/3 according to the table 2.1 shown in the previous section 2.3.3.

The SIMULINK model for induction motor is developed by using above equations and simulated successfully. The simulink model is given in figure 2.6 and induction motor sub block model also presented in figure 2.7. The wave forms of stator current in stationary and rotating reference frames and induction motor torque and speed waveforms given in figures

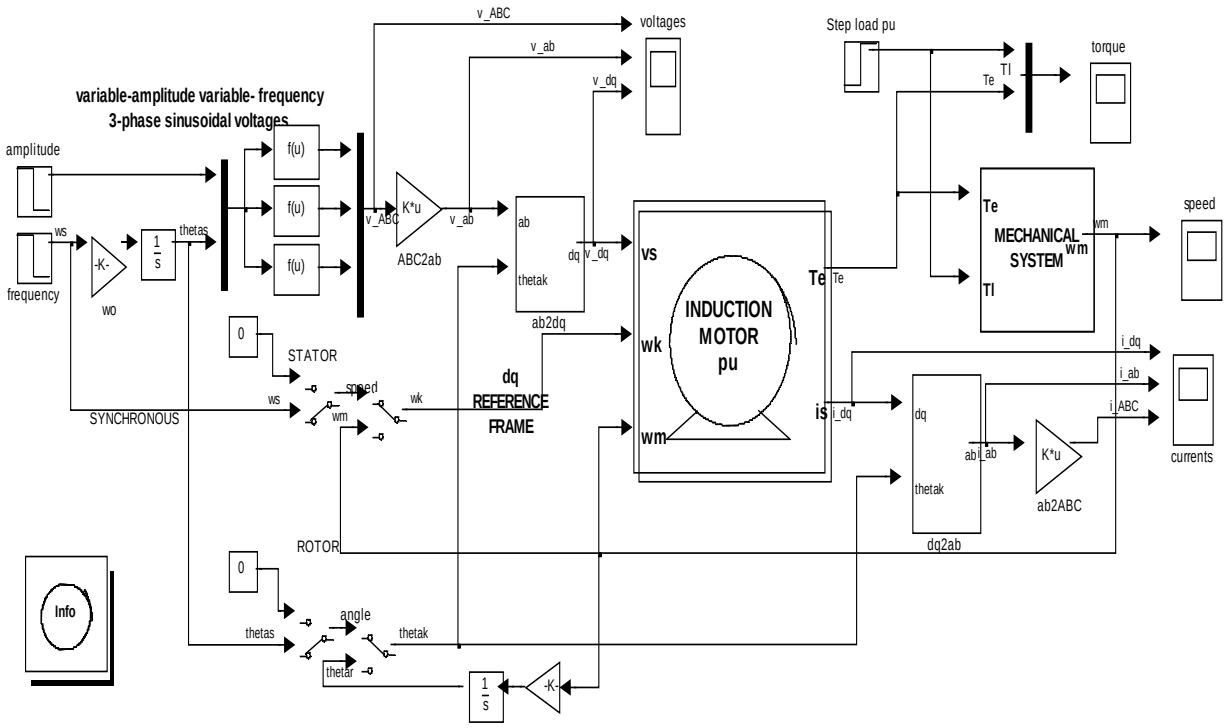

Fig 2.6. SIMULINK model for induction motor to obtain currents and voltages in different frames of references

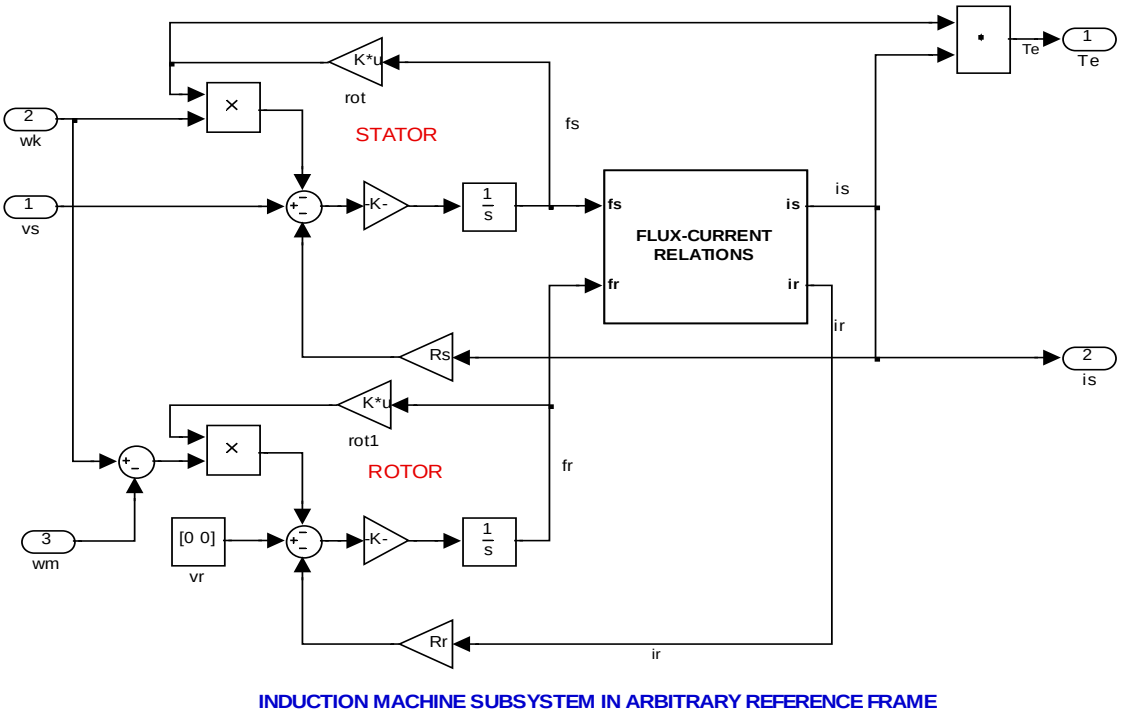

Fig 2.7.Induction machine subsystem modeled by using modeling equations

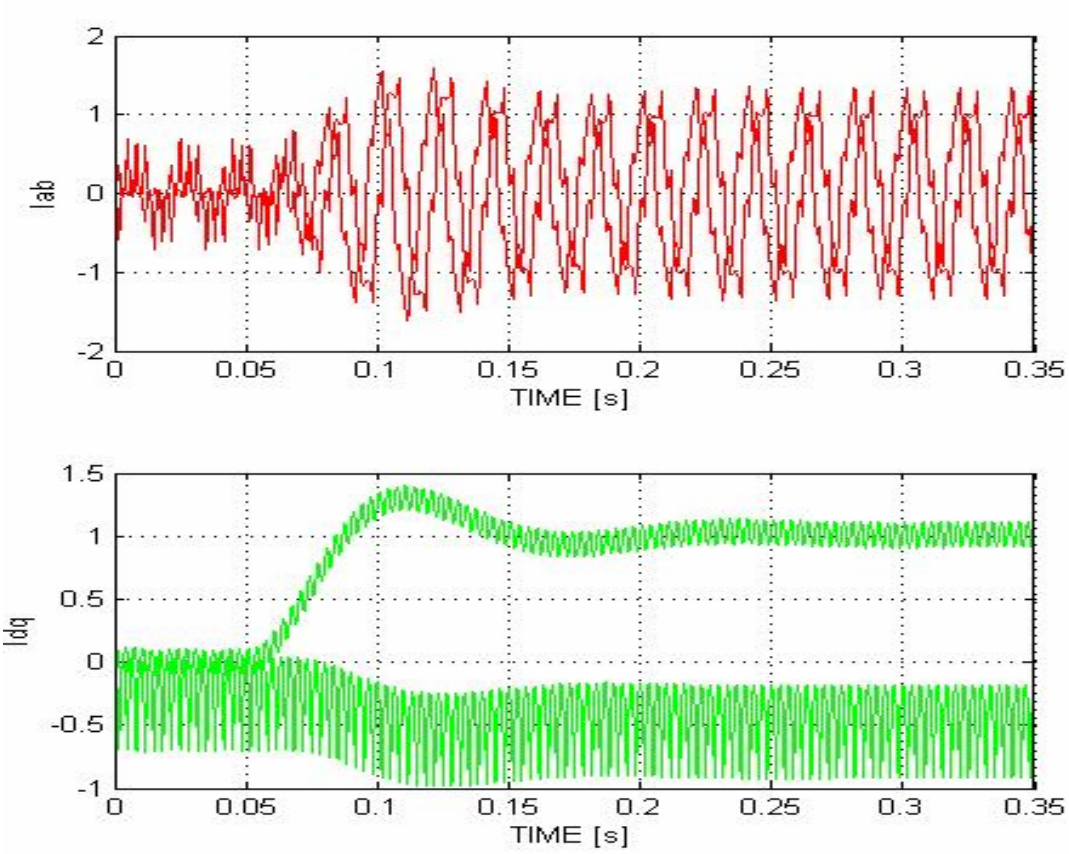

Fig 2.8 Induction motor stator current in stationary and rotating reference frames

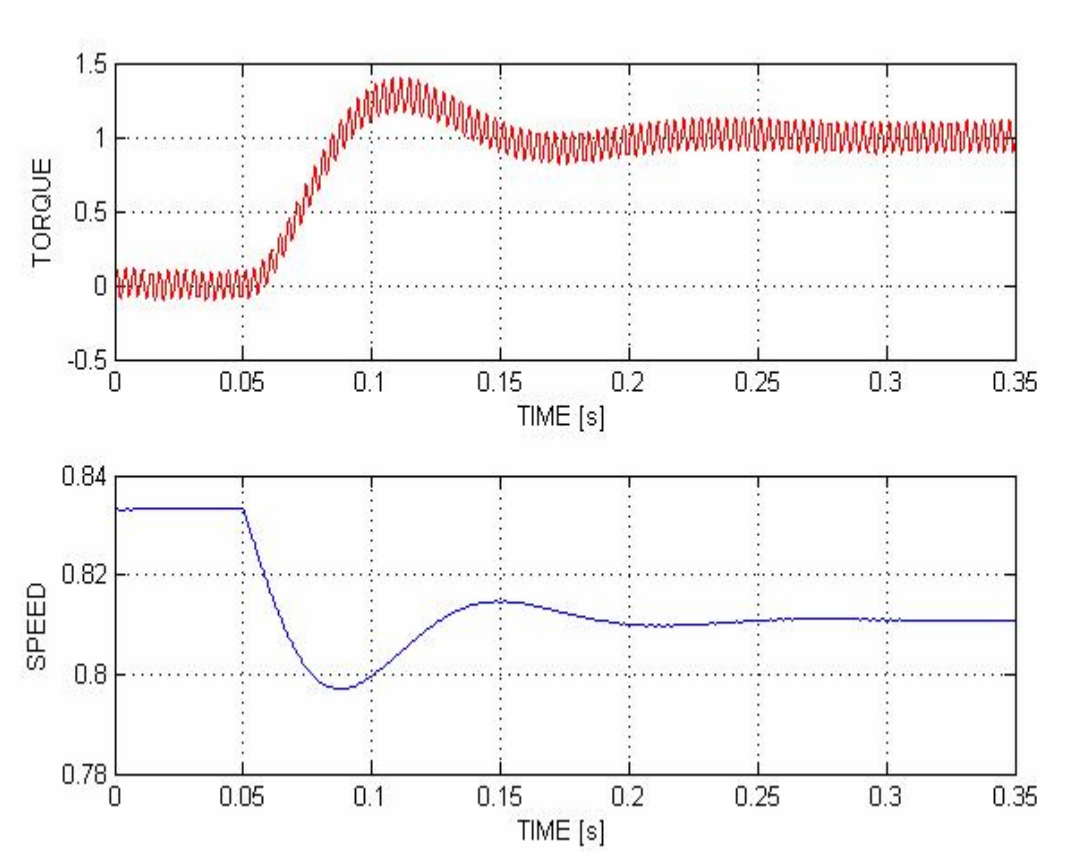

Fig 2.9.Torque and speed waveforms of induction motor

2.5 INTERIM CONCLUSIONS:

In the present chapter I have deduced the motor model. The model has been formulated by means of the two-axis theory equations and the space phasor notation. Despite the fact that both nomenclatures are valid, it has been proved that the space phasor notation is much more compact and easier to work with. The model has been developed in both nomenclatures for the stator, rotor and synchronous references. In further chapters, the motor model with stator reference, introduced in section 2.4.1.1, will be the one most used. The final concrete equations used in the MATLAB/SIMULINK motor model have been presented by the three different references. Some simulations are shown to prove the validity of the model, being equal for the previously mentioned three references. Finally the steady state motor analysis has been introduced.

Chapter 3

DIRECT TORQUE CONTROL OF INDUCTION MOTOR

Introduction

DTC controller

DTC schematic

SIMULINK Model

Interim Conclusions

DIRECT TORQUE CONTROL OF INDUCTION MOTORS

3.1 INTRODUCTION:

3.1.1 DC drive analogy:

In a dc machine, neglecting the armature reaction effect and field saturation, the developed torque is given by

$$T_e = K_a . I_a . I_f \quad \text{--------- (3.1)}$$

Where I_a = armature current and I_f = field current.

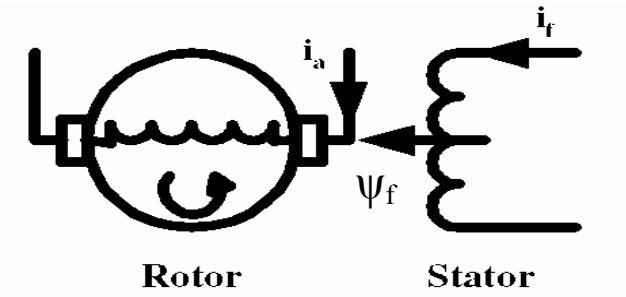

Fig 3.1 DC motor model

The construction of a DC machine is such that the field ψ_f produced by the current I_f is perpendicular to the armature flux ψ_a, which is produced by the armature current I_a. These space vectors, which are stationary in space, are orthogonal or decoupled in nature as shown in figure 3.1. This means that when torque is controlled by controlling the current I_a, the flux ψ_f is not effected and we get the fast transient response and high torque/ampere ratio with the rated ψ_f. Because of the decoupling, when the field current I_f is controlled, it affects the field flux ψ_f only, but not the ψ_a flux.

The DC machine like performance is obtained in Direct Torque Controlled (DTC) drives. In DTC drives, the de-coupling of the torque and flux components is accomplished by using hysteresis comparators which compares the actual and estimated values of the electromagnetic torque and stator flux. The DTC drive consists of DTC controller, torque and flux calculator, and a Voltage Source Inverter (VSI).

3.1.2 Principle of direct torque control of induction motor:

Direct torque control was developed by Takahashi [1] and Depenbrock [13] as an alternative to field-oriented control [3], [15]. In a direct torque controlled (DTC) induction motor drive supplied by a voltage source inverter, it is possible to control directly the stator flux linkage ψ_s (or the rotor flux ψ_r or the magnetizing flux ψ_m) and the electromagnetic torque by the selection of an optimum inverter voltage vector. The selection of the voltage vector of the voltage source inverter is made to restrict the flux and torque error within their respective flux and torque hysteresis bands and to obtain the fastest torque response and highest efficiency at every instant. DTC enables both quick torque response in the transient operation and reduction of the harmonic losses and acoustic noise.

As it has been introduced in expression 2.64, the electromagnetic torque in the three phase induction machines can be expressed as follows [3]:

$$t_e = \frac{3}{2} P \overline{\psi}_s \times \overline{i}_s \qquad \text{--------- (3.2)}$$

Where ψ_s is the stator flux, i_s is the stator current (both fixed to the stationary reference frame fixed to the stator) and P the number of pairs of poles. The previous equation can be modified and expressed as follows:

$$t_e = \frac{3}{2} P \left|\overline{\psi_s}\right| \times \left|\overline{i_s}\right| . \sin\left(\alpha_s - \rho_s\right) \qquad \text{--------- (3.3)}$$

Where ρ_s is the stator flux angle and α_s is the stator current one, both referred to the horizontal axis of the stationary frame fixed to the stator. If the stator flux modulus is kept constant and the angle ρ_s is changed quickly, then the electromagnetic torque is directly controlled. The same conclusion can be obtained using another expression for the electromagnetic torque. From equation 1.83, next equation can be written:

$$t_e = \frac{3}{2} P \frac{L_m}{L_s L_r - L_m^2} \left|\overline{\psi_r}'\right| \times \left|\psi_s\right| . \sin\left(\rho_s - \rho_r\right) \qquad \text{--------- (3.4)}$$

Because of the rotor time constant is larger than the stator one, the rotor flux changes slowly compared to the stator flux; in fact, the rotor flux can be assumed constant. (The fact that the rotor flux can be assumed constant is true as long as the response time of the control is much faster than the rotor time constant). As long as the stator flux modulus is kept constant, then the electromagnetic torque can be rapidly changed and controlled by means of changing the angle $\rho_s - \rho_r$ [16] [3].

3.2 - DTC CONTROLLER:

The way to impose the required stator flux is by means of choosing the most suitable Voltage Source Inverter state. If the ohmic drops are neglected for simplicity, then the stator voltage impresses directly the stator flux in accordance with the following equations

$$\frac{d\,\overline{\psi}_s}{d\,t} = \overline{V}_s$$

Or: --------- (3.5)

$$\Delta\overline{\psi}_s = \overline{Vs}.\Delta t$$

Decoupled control of the stator flux modulus and torque is achieved by acting on the radial and tangential components respectively of the stator flux-linkage space vector in its locus. These two components are directly proportional (Rs=0) to the components of the same voltage space vector in the same directions. So imposing of proper voltage vector is important in direct torque control of induction motor. This we will obtained by using voltage source inverter.

3.3.1 Voltage Source Inverter

There are many topologies for the voltage source inverter used in DTC control of induction motors that give high number of possible output voltage vectors [16], [17] but the most common one is the six step inverter. A six step voltage inverter provides the variable frequency AC voltage input to the induction motor in DTC method. The DC supply to the inverter is provided either by a DC source like a battery, or a rectifier supplied from a three phase (or single phase) AC source. Fig. 3.2 shows a six step voltage source inverter. The inductor L is inserted to limit shot through fault current. A large electrolytic capacitor C is inserted to stiffen the DC link voltage.

The switching devices in the voltage source inverter bridge must be capable of being turned off and on. Insulated gate bipolar transistors (IGBT) are used because they have this ability in addition; they offer high switching speed with enough power rating. Each IGBT has an inverse parallel-connected diode. This diode provide alternate path for the motor current after the IGBT, is turned off [5].

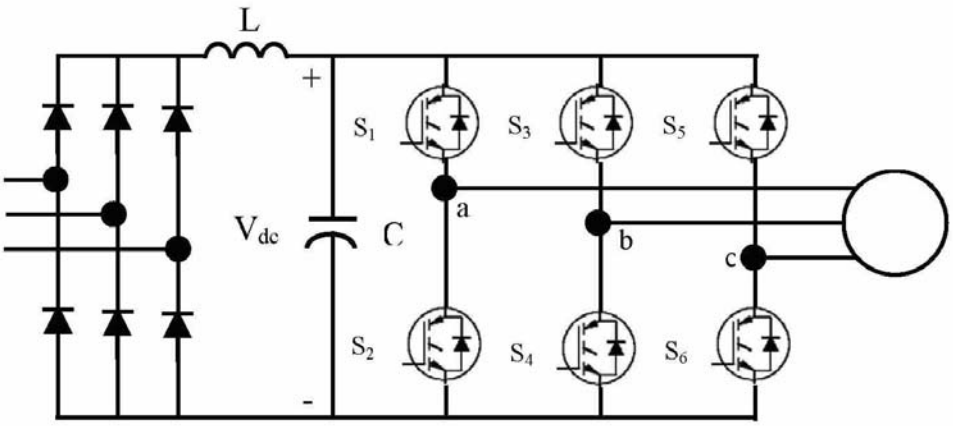

Fig 3.2 Voltage Source Inverter

Each leg of the inverter has two switches one connected to the high side (+) of the DC link and the other to the low side (-); only one of the two can be on at any instant. When the high side gate signal is on the phase is assigned the binary number 1, and assigned the binary number 0 when the low side gate signal is on. Considering the combinations of status of phases a, b and c the inverter has eight switching modes ($V_aV_bV_c$=000-111) two are zero voltage vectors V_0 (000) and V_7 (111) where the motor terminals is short circuited and the others are nonzero voltage vectors V_1 to V_6

The dq model for the voltage source inverter in the stationary reference frame is obtained by applying the dq transformation Equation to the inverter switching modes. The six nonzero voltages space vectors will have the orientation shown in Fig. 2.6, and also shows the possible dynamic locus of the stator flux, and its different variation depending on the VSI states chosen. The possible global locus is divided into six different sectors signaled by the discontinuous line. Each vector lies in the center of a sector of 60^o width named S1 to S6 according to the voltage vector it contains.

From Equation 3.5 it can be seen that the inverter voltage directly force the stator flux, the required stator flux locus will be obtained by choosing the appropriate inverter switching state. Thus the stator flux linkage move in space in the direction of the stator voltage space vector at a speed that is proportional to the magnitude of the stator voltage space vector. By selecting step by step the appropriate stator voltage vector, it is then possible to change the stator flux in the required way. If an increase of the torque is required then the torque is controlled by applying voltage vectors that advance the flux linkage space vector in the direction of rotation. If a decrease in torque is required then zero switching vector is applied, the zero vector that minimize inverter switching is selected. In summary if the stator flux vector lies in the k-th sector and the motor is running anticlockwise

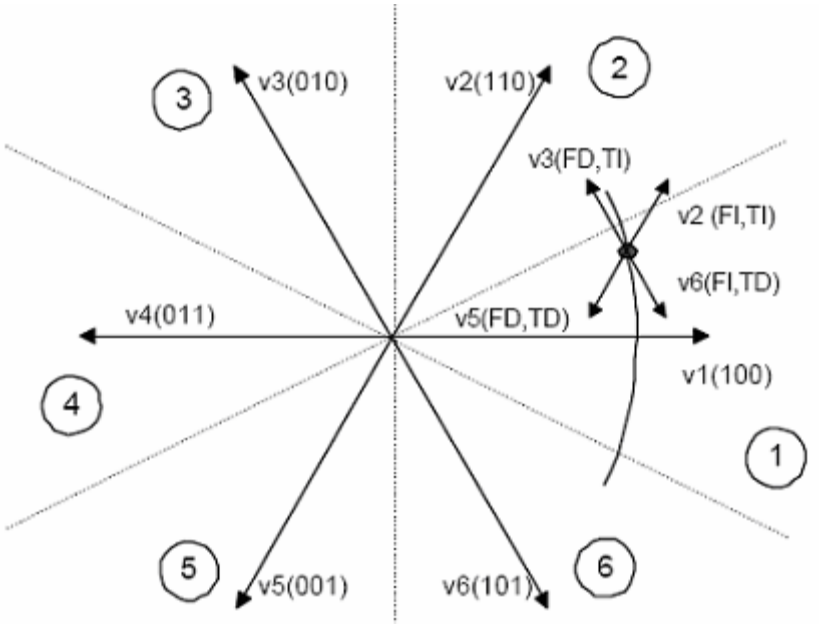

Fig 3.3.Stator flux vector locus and different possible switching
Voltage vectors. FD: flux decrease. FI: flux increase. TD: torque decrease.
TI: torque increase

then torque can be increased by applying stator voltage vectors V_{k+1} or V_{k+2}, and decreased by applying a zero voltage vector V_0 or V_7. Decoupled control of the torque and stator flux is achieved by acting on the radial and tangential components of the stator voltage space vector in the same directions, and thus can be controlled by the appropriate inverter switching. In general, if the stator flux linkage vector lies in the k-th sector its magnitude can be increased by using switching vectors V_{k-1} (for clockwise rotation) or V_{k+1} (for anticlockwise rotation), and can be decreased by applying voltage vectors V_{k-2} (for clockwise rotation) or V_{k+2} (for anticlockwise rotation). In Accordance with figure 2.1, the general table II.I can be written. It can be seen from table II.I, that the states Vk and Vk+3 , are not considered in the torque because they can both increase (first 30 degrees) or decrease (second 30 degrees) the torque at the same sector depending on the stator flux position.

VOLTAGE VECTOR	INCREASE	DECREASE
Stator Flux	V_k, V_{k+1}, V_{k-1}	$V_{k+2}, V_{k-2}, V_{k+3}$
Torque	V_{k+1}, V_{k+2}	V_{k-1}, V_{k-2}

Table3.1.General Selection Table for Direct Torque Control, "k" being the sector number.

This can be tabulated in the look-up Table 2.1 (Takahashi look-up table). Finally, the DTC classical look up table is as follows:

Flux Error $d\psi$	**Torque Error** dT	**S1**	**S2**	**S3**	**S4**	**S5**	**S6**
1	1	$\mathbf{V}_2$	$\mathbf{V}_3$	$\mathbf{V}_4$	$\mathbf{V}_5$	$\mathbf{V}_6$	V1
	0	V_0	$\mathbf{V}_7$	V_0	$\mathbf{V}_7$	V_0	$\mathbf{V}_7$
	-1	$\mathbf{V}_6$	V**i**	$\mathbf{V}_2$	$\mathbf{V}_3$	$\mathbf{V}_4$	$\mathbf{V}_5$
0	1	$\mathbf{V}_3$	$\mathbf{V}_4$	$\mathbf{V}_5$	$\mathbf{V}_6$	V1	$\mathbf{V}_2$
	0	V_0	$\mathbf{V}_7$	V_0	$\mathbf{V}_7$	V_0	$\mathbf{V}_7$
	-1	$\mathbf{V}_5$	$\mathbf{V}_6$	V1	$\mathbf{V}_2$	$\mathbf{V}_3$	$\mathbf{V}_4$

Table3.2 conventional DTC look up table

3.3 DTC SCHEMATIC:

In figure 1.2 a possible schematic of Direct Torque Control is shown. As it can be seen, there are two different loops corresponding to the magnitudes of the stator flux and torque. The reference values for the flux stator modulus and the torque are compared with the actual values, and the resulting error values are fed into the twolevel and three-level hysteresis blocks respectively. The outputs of the stator flux error and torque error hysteresis blocks, together with the position of the stator flux are used as inputs of the look up table (see table II.II). The inputs to the look up table are given in terms of +1,0,-1 depend on weather the torque and flux errors within or beyond hysteresis bands and the sector number in which the flux sector presents at that particular instant. In accordance with the figure 1.2, the stator flux modulus and torque errors tend to be restricted within its respective hysteresis bands.

From the schematic of DTC it is cleared that, for the proper selection of voltage sector from lookup table, the DTC scheme require the flux and torque estimations.

3.3.1 Methods for Estimation of Stator Flux in DTC:

Accurate flux estimation in Direct Torque controlled induction motor drives is important to ensure proper drive operation and stability. Most of the flux estimation techniques proposed is based on voltage model, current model, or the combination of both [18]. The estimation based on current model normally applied at low frequency, and

it requires the knowledge of the stator current and rotor mechanical speed or position. In some industrial applications, the use of incremental encoder to get the speed or position of the rotor is undesirable since it reduces the robustness and reliability of the drive. It has been widely known that even though the current model has managed to eliminate the sensitivity to the stator resistance variation. The use of rotor parameters in the estimation introduced error at high rotor speed due to the rotor parameter variations. So in this present DTC control scheme the flux and torque are estimated by using voltage model described by equations 3.6-3.8, which does not need a position sensor and the only motor parameter used is the stator resistance.

$$\psi_{sD} = \int \left(V_{sD} - R_s I_{sD}\right) dt = i_{sD} \cdot \frac{L_x}{L_m} + \psi'_{rd} \cdot \frac{L_m}{L_r} \quad \text{--------- (3.6)}$$

$$\psi_{sQ} = \int \left(V_{sQ} - R_s I_{sQ}\right) dt = i_{sQ} \cdot \frac{L_x}{L_m} + \psi'_{rq} \cdot \frac{L_m}{L_r} \quad \text{--------- (3.7)}$$

Where $L_x = L_s L_r - L_m{}^2$ and i_{sD} , i_{sQ} are calculated by using equations……..

And torque can be estimated by equation

$$t_e = \frac{3}{2} P \left(\psi_{sD} . i_{sQ} - \psi_{sQ} . i_{sD}\right) \quad \text{--------- (3.8)}$$

By using these estimated values from voltage model we proceed to the lookup table to select the proper voltage vector The voltage model gives accurate estimation at high speeds however, at low speed, some problems arise. In practical implementation, even a small DC off-set present in the back emf due to noise or measurement error inherently present in the current sensor, can cause the integrator to saturate [3].

3.4 SIMULINK MODEL FOR CONVENTIONAL DTC:

A SIMULINK model is developed by using the induction motor model presented in figure 3.3 and also MATLAB programme is developed for the implementation of conventional DTC. The simulink model for the conventional DTC is developed and is simulated. The waveform for induction motor torque, which is obtained from simulation of MATLAB programme is presented and verified with SIMULINK waveforms.

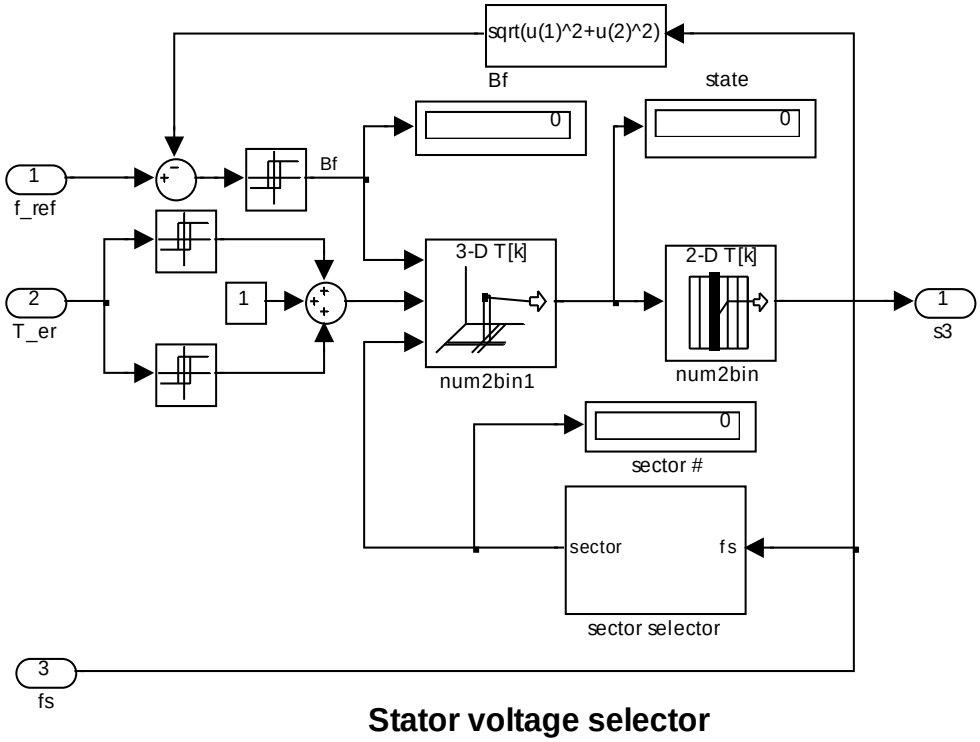

Fig 3.4 SIMULINK model for conventional DTC

A three dimensional matrix is developed by MATLAB programme which is called by simulink model during the simulation and is given by

%switching table for DTC

```
clc,clear
a(:,:,1) =[1 0 2;5 7 6];
a(:,:,2) =[5 7 3;4 0 2];
a(:,:,3) =[4 0 1;6 7 3];
a(:,:,4) =[6 7 5;2 0 1];
a(:,:,5) =[2 0 4;3 7 5];
a(:,:,6) =[3 7 6;1 0 4];
a
```

The waveform for torque of the induction motor with the application of load torque of 1.5N.m is given in figure 3.4, which is obtained from simulation of MATLAB programme with a sampling time of 0.0002. It indirectly means that the drive output is updated at a rate of 5 KHz.

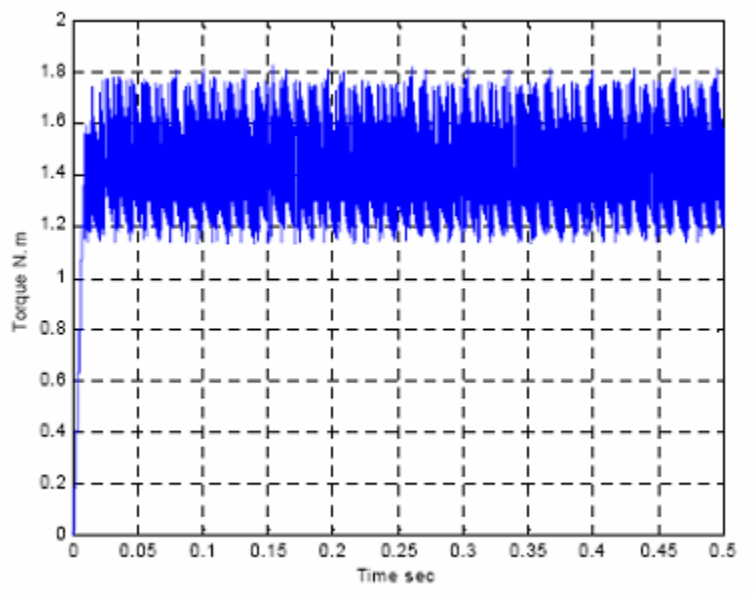

Fig 3.5 Electric torque waveform for conventional DTC

3.5 INTERIM CONCLUSIONS:

From the torque waveform obtained from simulation of conventional DTC, it is cleared that the torque ripple is 0.6 Nm (approximately 1.8-1.2 Nm maximum and minimum values respectively) with the conventional DTC.

This high magnitude of torque ripple is the main drawback of conventional DTC. The other drawbacks also summarized as follows:

- Large and small errors in flux and torque are not distinguished. In other words, the same vectors are used during start up and step changes and during steady state.
- Sluggish response (slow response) in both start up and changes in either flux or torque.

In order to overcome the mentioned drawbacks, there are different solutions, like Non artificial intelligence methods, mainly "sophisticated tables" and fuzzy logic based systems.

In the next sections of my thesis work deal with DTC with the duty ratio fuzzy control to minimize torque ripple and realized the best DTC improvement.

Chapter 4

FUZZY LOGIC CONTROLLERS

Introduction to FLC

Why Fuzzy Logic Controllers

Fuzzy Logic Controller

FUZZYLOGIC CONTROLLERS

4.1 Introduction to FLC

Fuzzy logic has rapidly become one of the most successful of today's technology for developing sophisticated control system. With it aid complex requirement so may be implemented in amazingly simple, easily minted and inexpensive controllers. The past few years have witnessed a rapid growth in number and variety of application of fuzzy logic. The application range from consumer products such as cameras ,camcorder ,washing machines and microwave ovens to industrial process control ,medical instrumentation ,and decision-support system .many decision-making and problem solving tasks are too complex to be understand quantitatively however ,people succeed by using knowledge that is imprecise rather than precise . fuzzy logic is all about the relative importance of precision .fuzzy logic has two different meanings .in a narrow senses ,fuzzy logic is a logical system which is an extension of multi valued logic .but in wider sense fuzzy logic is synonymous with the theory of fuzzy sets . Fuzzy set theory is originally introduced by Lotfi Zadeh in the 1960,s resembles approximate reasoning in it use of approximate information and uncertainty to generate decisions.

Several studies show, both in simulations and experimental results, that Fuzzy Logic control yields superior results with respect to those obtained by conventional control algorithms thus, in industrial electronics the FLC control has become an attractive solution in controlling the electrical motor drives with large parameter variations like machine tools and robots. However, the FL Controllers design and tuning process is often complex because several quantities, such as membership functions, control rules, input and output gains, etc must be adjusted. The design process of a FLC can be simplified if some of the mentioned quantities are obtained from the parameters of a given Proportional-Integral controller (PIC) for the same application.

4.2 Why fuzzy logic controller (FLC)

- Fuzzy logic controller is used to design nonlinear systems in control applications.

The design of conventional control system essential is normally based on the mathematical model of plant .if an accurate mathematical model is available with known parameters it can be analyzed., for example by bode plots or nyquist plot , and controller can be designed for specific performances .such procedure is time consuming[18].

- Fuzzy logic controller has adaptive characteristics.

The adaptive characteristics can achieve robust performance to system with uncertainty parameters variation and load disturbances.

4.3. Fuzzy logic controller (FLC)

Fuzzy logic expressed operational laws in linguistics terms instead of mathematical equations. Many systems are too complex to model accurately, even with complex mathematical equations; therefore traditional methods become infeasible in these systems. However fuzzy logics linguistic terms provide a feasible method for defining the operational characteristics of such system [18].

Fuzzy logic controller can be considered as a special class of symbolic controller. The configuration of fuzzy logic controller block diagram is shown in Fig.4.1

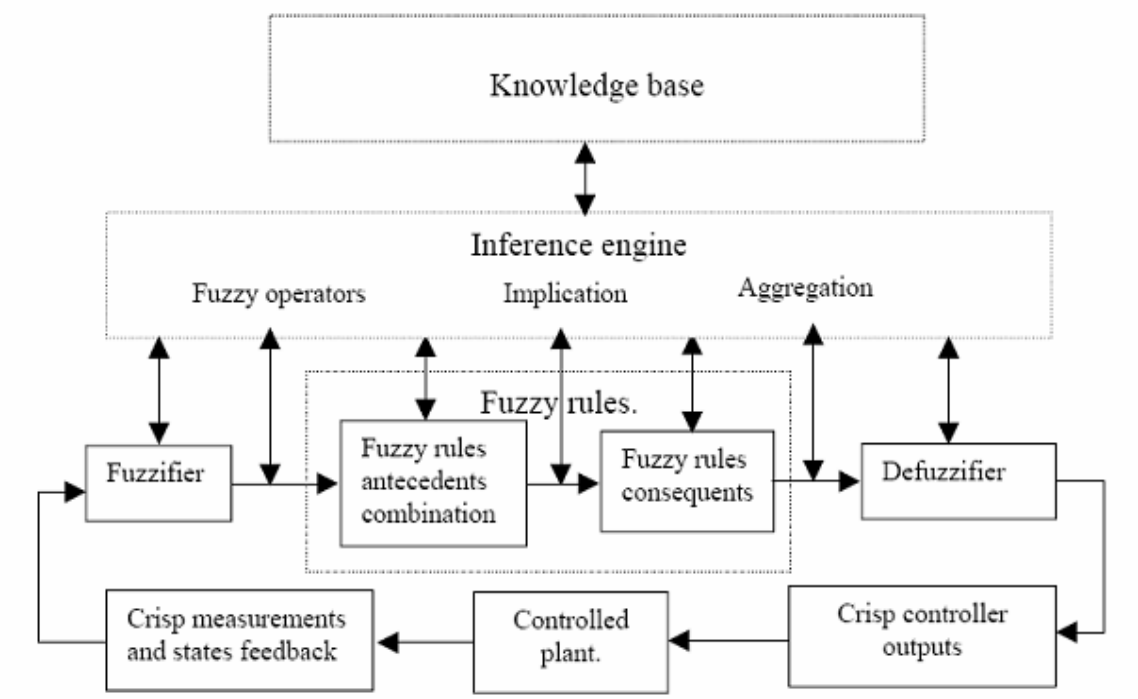

Fig 4.1 Block diagram for Mamdani type Fuzzy Logic Controller

The fuzzy logic controller has three main components

1. Fuzzification.
2. Fuzzy inference.
3. Defuzzification.

4.3.1. Fuzzification

The following functions:

1. Multiple measured crisp inputs first must be mapped into fuzzy membership function this process is called fuzzification.
2. Performs a scale mapping that transfers the range of values of input variables into corresponding universes of discourse.
3. Performs the function of fuzzification that converts input data into suitable linguistic values which may be viewed as labels of fuzzy sets.

Fuzzy logic's linguistic terms are often expressed in the form of logical implication, such as *if-then* rules. These rules define a range of values known as fuzzy member ship functions. Fuzzy membership function may be in the form of a triangle, a trapezoidal, a bell (as shown in Fig.4.2) or another appropriate from [18].

The triangle membership function is defined in (4.1).Triangle membership functions limits defined by V_{al1}, V_{al2} and V_{al3}.

$$\mu(u_i) = \begin{cases} \dfrac{u_i - V_{al1}}{V_{al2} - V_{al1}}, V_{al1} \le u_i \le V_{al2} \\ \dfrac{V_{al3} - u_i}{V_{al3} - V_{al2}}, V_{al2} \le u_i \le V_{al2} \\ 0, \qquad\quad othetrwise \end{cases} \tag{4.1}$$

Trapezoid membership function defined in (4.2) .Trapezoid membership functions limits are defined by V_{al1}, V_{al2}, V_{al3} and V_{al4}.

$$\mu_i(u_i) = \begin{cases} \dfrac{u_i - V_{al1}}{V_{al2} - V_{al1}}, V_{al1} \le u_i \le V_{al2} \\ 1, \qquad\quad , V_{al2} \le u_i \le V_{al3} \\ \dfrac{V_{al4} - u_i}{V_{al4} - V_{al3}}, V_{al3} \le u_i \le V_{al4} \\ 0 \qquad\quad , otherwise \end{cases} \tag{4.2}$$

The bell membership functions are defined by parameters X_p, w and m as follows:

$$\mu(u_i) = \frac{1}{\left(1 + \left(\dfrac{|u_i - X_p|}{w}\right)^{2m}\right)} \tag{4.3}$$

Where X_p the midpoint and w is the width of bell function. $m \ge 1$, and describe the convexity of the bell function.

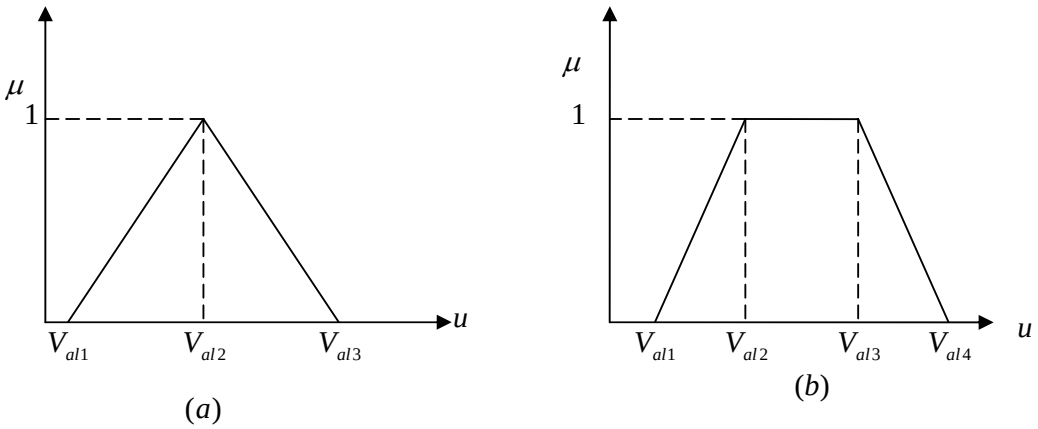

(*a*) (*b*)

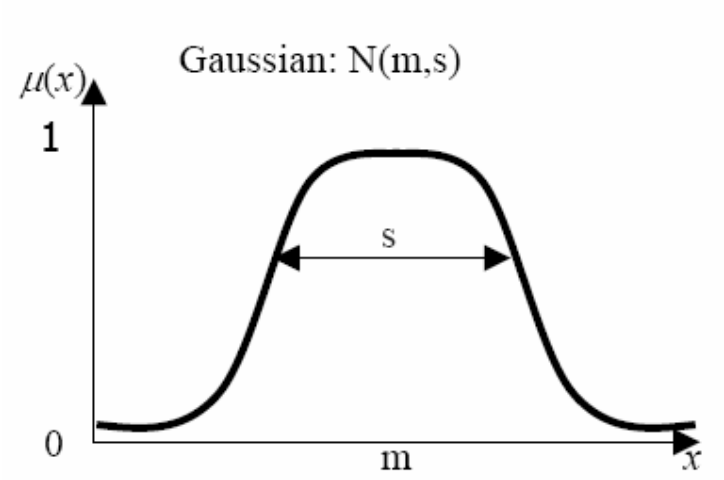

(c)

Fig.4.2. (a) Triangle, (b) Trapezoid, and (c) Gaussian membership functions.

The inputs of the fuzzy controller are expressed in several linguist levels. As shown in Fig.4.3 these levels can be described as positive big (PB), positive medium (PM), positive small (PS) negative small (NS), negative medium (NM), negative big(NB) or in other levels. Each level is described by fuzzy set [18].

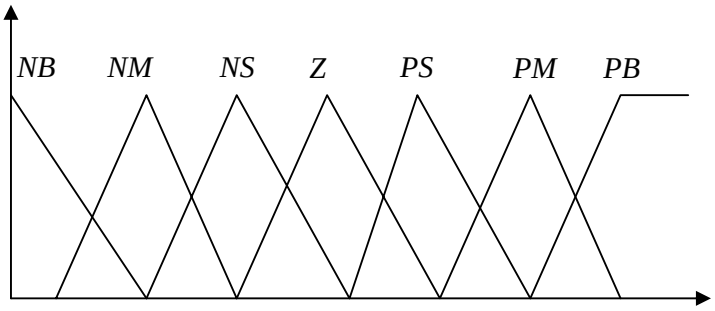

Figure.4.3.Seven levels of fuzzy membership function

4.3.2. Fuzzy inference

Fuzzy inference is the process of formulating the mapping from a given input to an output using fuzzy logic. The mapping then provides a basis from which decisions can be made, or patterns discerned. There are two types of fuzzy inference systems that can be implemented in the Fuzzy Logic Toolbox: Mamdani-type and Sugeno-type. These two types of inference systems vary somewhat in the way outputs are determined.

Fuzzy inference systems have been successfully applied in fields such as automatic control, data classification, decision analysis, expert systems, and computer vision. Because of its multidisciplinary nature, fuzzy inference systems are associated with a number of names, such as fuzzy-rule-based systems, fuzzy expert systems, fuzzy modeling, fuzzy associative memory, fuzzy logic controllers, and simply (and ambiguously) fuzzy

Mamdani's fuzzy inference method is the most commonly seen fuzzy methodology. Mamdani's method was among the first control systems built using fuzzy set theory. It was proposed in 1975 by Ebrahim M amdani [18] as an attempt to control a steam engine and boiler combination by synthesizing a set of linguistic control rules obtained from experienced human operators. Mamdani's effort was based on Lotfi Zadeh's 1973 paper on fuzzy algorithms for complex systems and decision processes [18].

The second phase of the fuzzy logic controller is its fuzzy inference where the knowledge base and decision making logic reside .The rule base and data base from the knowledge base. The data base contains the description of the input and output variables. The decision making logic evaluates the control rules .the control-rule base can be developed to relate the output action of the controller to the obtained inputs.

4.3.3. Defuzzification

The output of the inference mechanism is fuzzy output variables. The fuzzy logic controller must convert its internal fuzzy output variables into crisp values so that the actual system can use these variables [18]. This conversion is called defuzzification. One may perform this operation in several ways. The commonly used control defuzzification strategies are

(a).The max criterion method (MAX)

The max criterion produces the point at which the membership function of fuzzy control action reaches a maximum value.

(b) The height method

The centroid of each membership function for each rule is first evaluated. The final output U_0 is then calculated as the average of the individual centroids, weighted by their heights as follows:

$$U_O = \frac{\sum_{i=1}^{n} u_i \mu(u_i)}{\sum_{i=1}^{n} \mu(u_i)} \tag{4.4}$$

(c) .The centroid method or center of area method (COA)

The widely used centroid strategy generates the center of gravity of area bounded by the

$$\bar{y} = \frac{\int \mu_Y(y).y dy}{\int \mu_Y(y) dy} \tag{4.5}$$

membership function cure.

Chapter 5

TORQUE RIPPLE MINIMIZATION IN DTC DRIVES

Introduction

Duty Ratio Control

Design of Duty Ratio Fuzzy Controller

Interim Conclusions

TORQUE RIPPLE MINIMIZATION IN DTC DRIVES

5.1 Introduction:

Direct torque control has many promising features and advantages such as absence of speed and position sensors, absence of coordinate transformation, reduced number of controllers and minimal torque response time. In addition, there are many limitations that need to be investigated. A major concern in direct torque control of induction motor drives is torque and flux ripples, since none of the inverter switching vectors is able to generate the exact stator voltage required to produce the desired changes in torque and flux. Possible solutions involve the use of high switching frequency or alternative inverter topologies. Increased switching frequency is desirable since it reduces the harmonic content of the stator currents, and reduces torque ripple. However, high switching frequency results in significantly increased switching losses leading to reduced efficiency and increased stress on the inverter semiconductor devices. Furthermore, in the case of high switching frequency, a fast processor is required since the control processing time becomes small. When an alternative inverter topology is used [16], it is possible to use an increased number of switches, but this also increases the cost. However, if instead of applying a voltage vector for the entire switching period, it is applied for a portion of the switching period, then the ripple can be reduced. This is defined as duty ratio control in which the ratio of the portion of the switching period for which a non-zero voltage vector is applied to the complete switching period is known as the duty ratio (δ).

5.2 Duty Ratio Control:

In the conventional DTC a voltage vector is applied for the entire switching period, and this causes the stator current and electromagnetic torque to increase over the whole switching period. Thus for small errors, the electromagnetic torque exceeds its reference value early during the switching period, and continues to increase, causing a high torque ripple. This is then followed by switching cycles in which the zero switching vectors are applied in order to reduce the electromagnetic torque to its reference value.

The ripple in the torque and flux can be reduced by applying the selected inverter vector not for the entire switching period, as in the conventional DTC induction motor drive, but only for part of the switching period. The time for which a non-

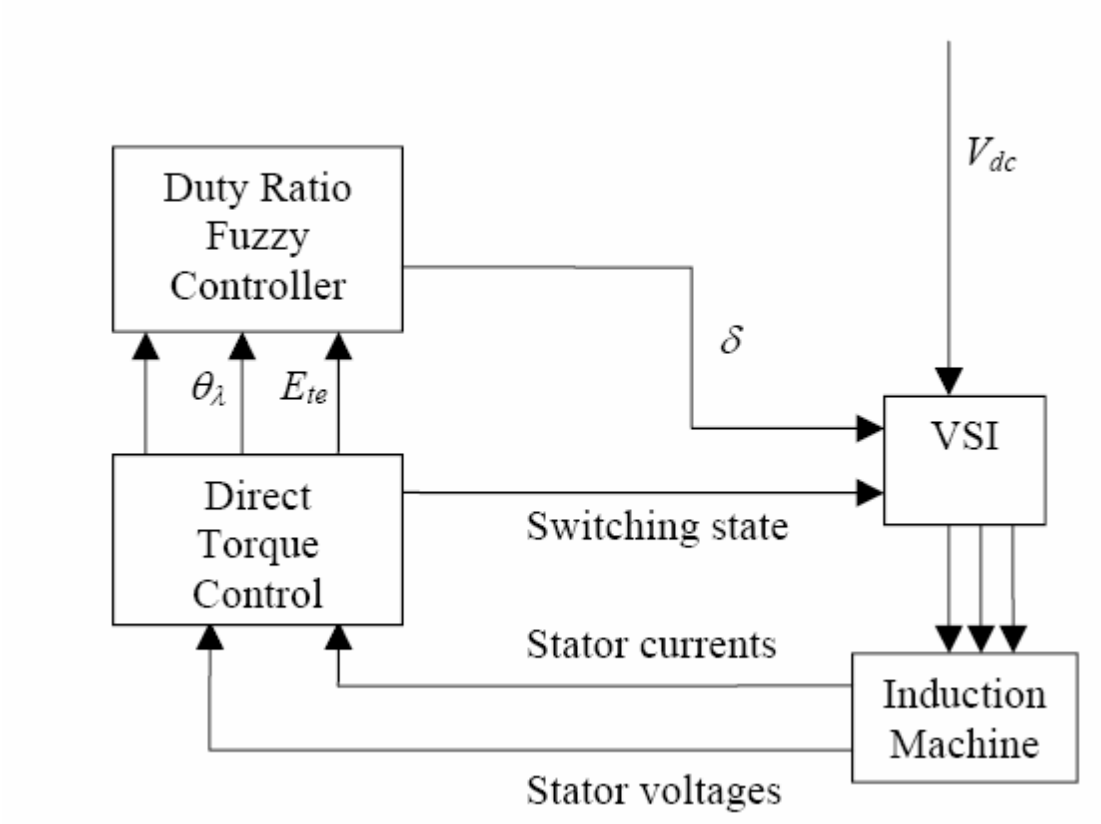

Fig 5.1 Block diagram for DTC with duty ratio fuzzy controller

-zero voltage vector has to be applied is chosen just to increase the electromagnetic torque to its reference value and the zero voltage vector is applied for the rest of the switching period as in Fig. 1.3(b). During the application of the zero voltage vector no power is absorbed by the machine, and thus the electromagnetic flux is almost constant; it only decreases slightly. Fig. 5.1 shows a DTC induction motor drive with a duty ratio fuzzy logic controller. The average input DC voltage to the motor during the application of each switching vector is δV_{dc}. By varying the duty ratio between zero and one, it is possible to apply voltage to the motor with an average value between 0 and V_{dc} during each switching period. Thus, the torque ripple will be less compared to applying the full DC link voltage for the complete switching period. This increases the choice of the voltage vector, without an increase in the number of semiconductor switches in the inverter.

The duty ratio of each switching period is a non-linear function of the electromagnetic torque error, stator flux-linkage error, and the position of the stator flux-linkage space vector. Thus, it is difficult to model this non-linear function. However, by using a fuzzy-logic-based DTC system, it is possible to perform fuzzy-logic-based duty-ratio control, where the duty ratio is determined during every switching cycle. In such a fuzzy-

logic system, there are three inputs, the electromagnetic torque error (E_{te}=T_{ref} -T), the stator flux-linkage space vector position (θ_{ψ}) within each sector associated with the voltage vectors as in Fig. 3.3 and the sign of the flux error (sign(E_{ψ})) where ($E_{\psi}=\psi_{ref}-\psi$). The output of the fuzzy-logic controller is the duty ratio (δ).

5.3 Design of the Duty Ratio Fuzzy Controller

There are many types of fuzzy logic controller for this particular application. A Mamdani-type fuzzy logic controller, which contains a rule base, a fuzzifier, and a defuzzifier, is chosen. Fuzzification is performed using membership function. The inputs and the output of the fuzzy controller are assigned Gausian membership functions as shown in Figs. 5.2-5.4. The universe of discourse for the torque error and the duty ratio is adjusted using simulations to get optimal torque ripple reduction. There are three groups of membership function depicted in Figures 5.2-5.4 corresponding to three input variables.

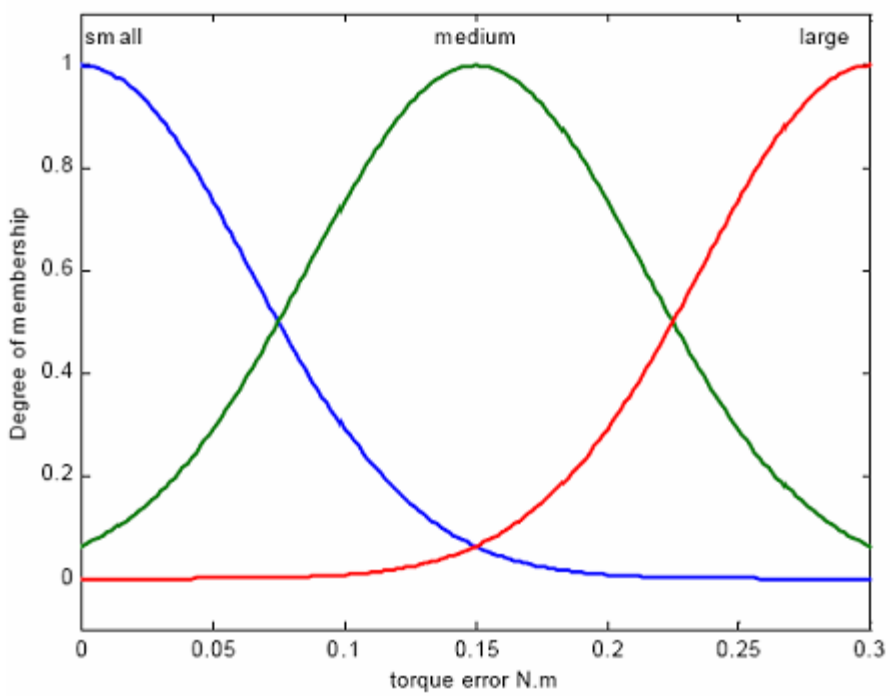

Fig 5.2 Membership functions distribution for the torque error (input)

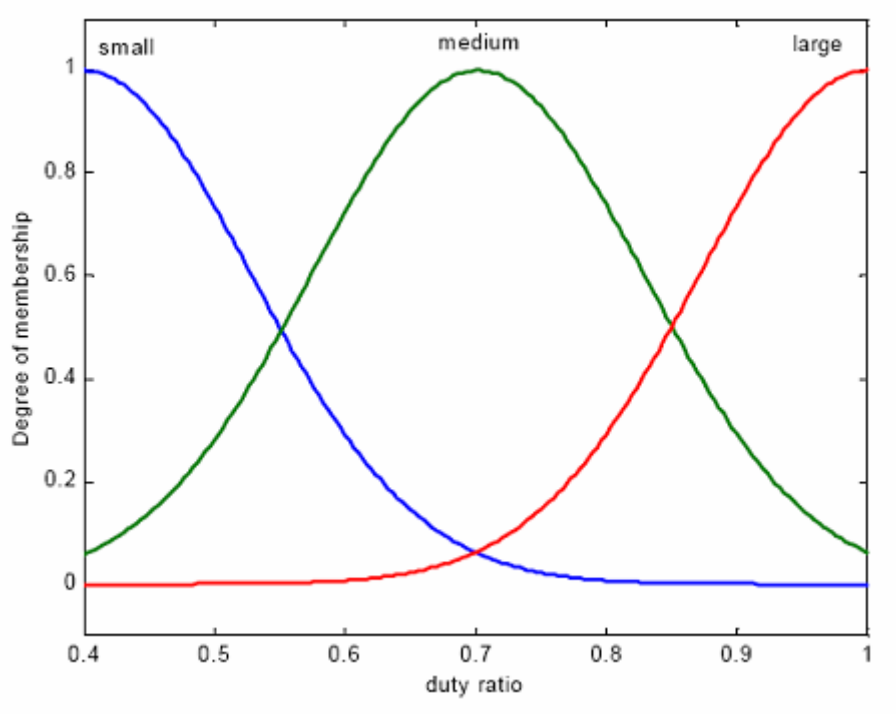

Fig 5.3 Membership functions distribution of the flux position (input)

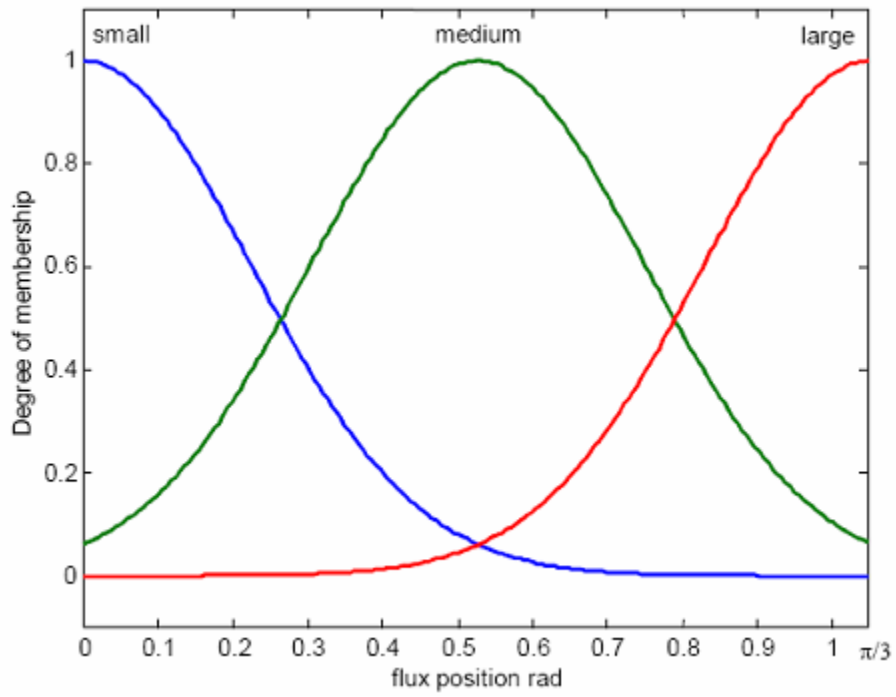

Fig 5.4 Membership functions distribution for duty ratio (output)

For the purpose of reducing the total rule numbers the fuzzy subset corresponding to the input θ' only covers the partial universe (0-Π/3) not like that of [19][21][22] which covers the whole universe. In [19][21][22] there are 180 rules altogether, which is too much to be incorporated into Fuzzy Logic Toolbox and is difficult to implement with hardware as well.

Based on the symmetry of impressed PWM voltage vector and flux angle in d-q coordinate, we define a mapping to convert the θ' in the range of (0-2.Π) into a sector with range of 0-$\pi/3$ [20].

$$\theta = \theta' - \frac{\pi}{3}\left[\frac{\theta' + \frac{\pi}{6}}{\frac{\pi}{3}}\right]$$

Where θ', the original angle of the stator is is is flux sector and θ is the actual angle that goes into fuzzy logic controller.

The emphasis in the fuzzy rule is to reduce the torque ripple. Generally the duty ratio is proportional to the torque error, since the torque rate of change is proportional to the angle between the stator flux and the applied voltage vector, the duty ratio depends also on the flux position within each sector. The use of two fuzzy sets is due to the fact that when the stator flux is greater than its reference value a voltage vector that advance the stator flux vector by two sectors is applied which result in a higher rate of change for the torque compared to the application of a voltage vector that advance the stator flux vector by one sector when the stator flux linkage is less than its reference value.

The duty ratio is selected proportional to the magnitude of the torque error so if the torque error is small, medium or large then the duty ratio is small, medium or large respectively. The fuzzy rules are then adjusted and tuned to reflect the effects of the flux error and position. If the torque error is medium and the stator flux lies in sector k with a magnitude greater than its reference value (negative flux error) then the voltage vector V_{k+2} is selected. If the flux position is small that means there is a large angle between the flux and the selected voltage vector that makes the selected vector more effective in increasing the toque so the duty ratio is set as small rather than medium, the fuzzy rule is stated a

If (torque error is medium) and (flux position is small) then (duty ratio is small)
If (torque error is large) and (flux position is small) then (duty ratio is medium)

Using the above reasoning and simulation to find the fuzzy rules, the two sets of fuzzy rules are summarized in Table 5.1.

flux	Torque error dT=±1 / Fluxangle	Small	Medium	Large
Negative dλ=0	Small	Small	Small	Medium
	Medium	Small	Medium	Large
	Large	Small	Medium	Large
Positive dλ=1	Small	Small	Medium	Large
	Medium	Small	Medium	Large
	Large	Medium	Large	Large

Table 5.1Rules for the duty ratio fuzzy controller

MATLAB® fuzzy logic toolbox was used in the implementation of the duty ratio fuzzy controller. The Graphic User Interface (GUI) included in the toolbox was used to edit the membership functions for the inputs (the torque error and the flux position), the output (the duty ratio) as shown in Fig. 4.2-4 and the two sets of fuzzy rules summarized in Table 4.1. A Mamdani type fuzzy inference engine (as described in Chapter IV) was used in the simulation. The membership functions and the fuzzy rules were adjusted using the simulation until an optimal torque ripple reduction was achieved. Fig. 4.8 shows the general view of the fuzzy controller when the stator flux is greater than its reference value.

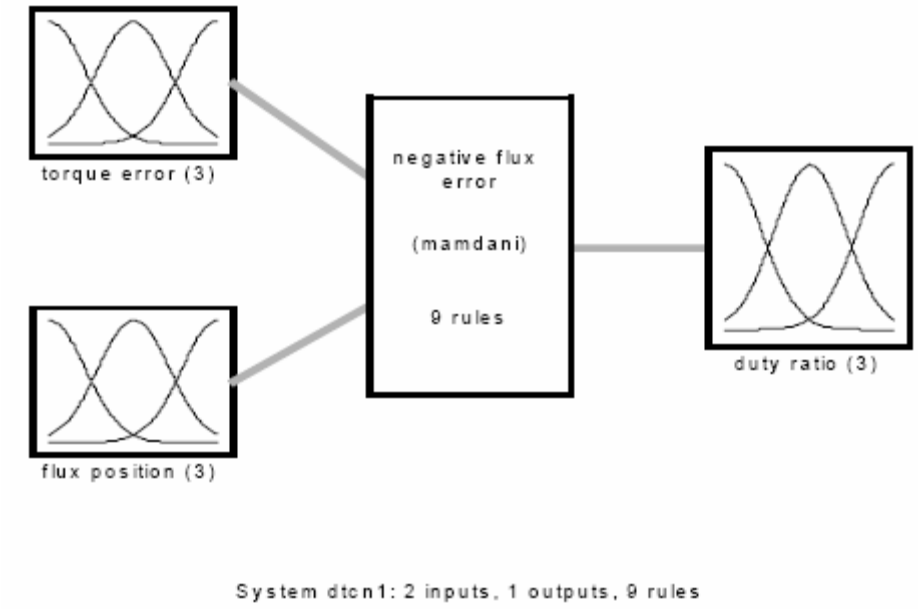

Fig 5.5 general view of duty ratio fuzzy controller

5.4 INTERIM CONCLUSIONS:

To examine the performance of the duty ratio controller the simulation was run at switching frequency 5 kHz. The difference between the conventional DTC and DTC with the duty ratio fuzzy control is clearly realized by examining the switching behavior of the stator voltage and the electric torque. Figure 5.6 contains voltage and torque switching in conventional DTC, where the drive output is updated at a rate of 5 kHz. The dotted vertical lines mark the beginnings of the sampling periods. It can be seen that the selected voltage vector is applied for the complete sampling period and the torque keeps increasing for the complete period; then a zero voltage is applied and the torque keeps decreasing for the complete sampling period and this results in high torque ripple.

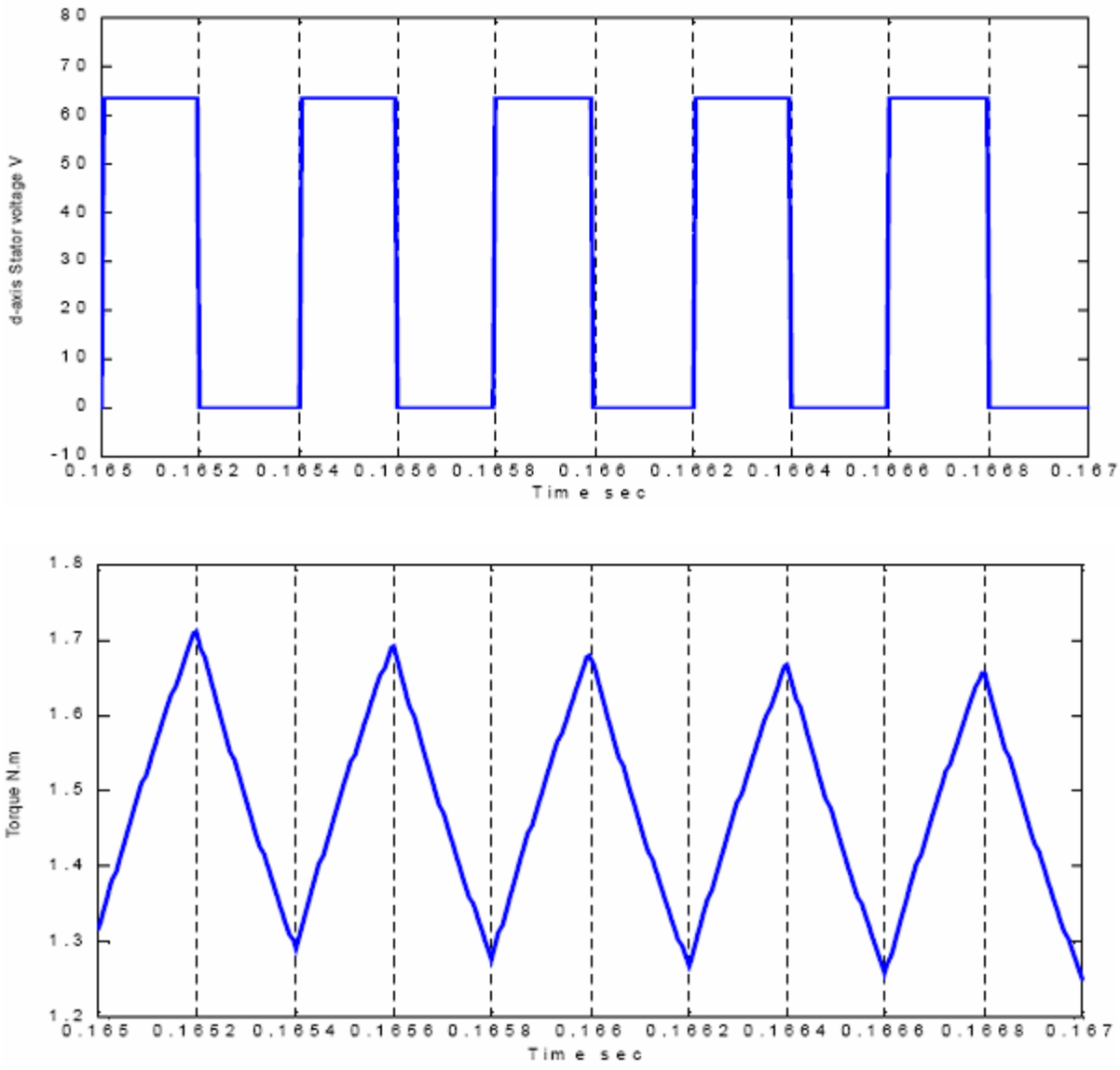

Fig 5.6 Voltage and torque switching in conventional DTC

In the DTC with the duty ratio fuzzy control as shown in Fig. 5.7, contains voltage and torque switching, where the drive output is updated at a rate of 5 kHz. The selected voltage vector is applied for part of the sampling period and removed for the rest of the period. As a result, the electric torque increases for part of the sampling period and then starts to decrease, this results in less torque ripple. By adjustment of the duty ratio, the desired average torque may be continuously maintained. The duty ratio controller smoothly adjusts the average stator voltage. There is no need to make coarse corrections by the use of multiple switching periods with a nonzero voltage vector or a whole switching period with a zero voltage vector as in the conventional DTC.

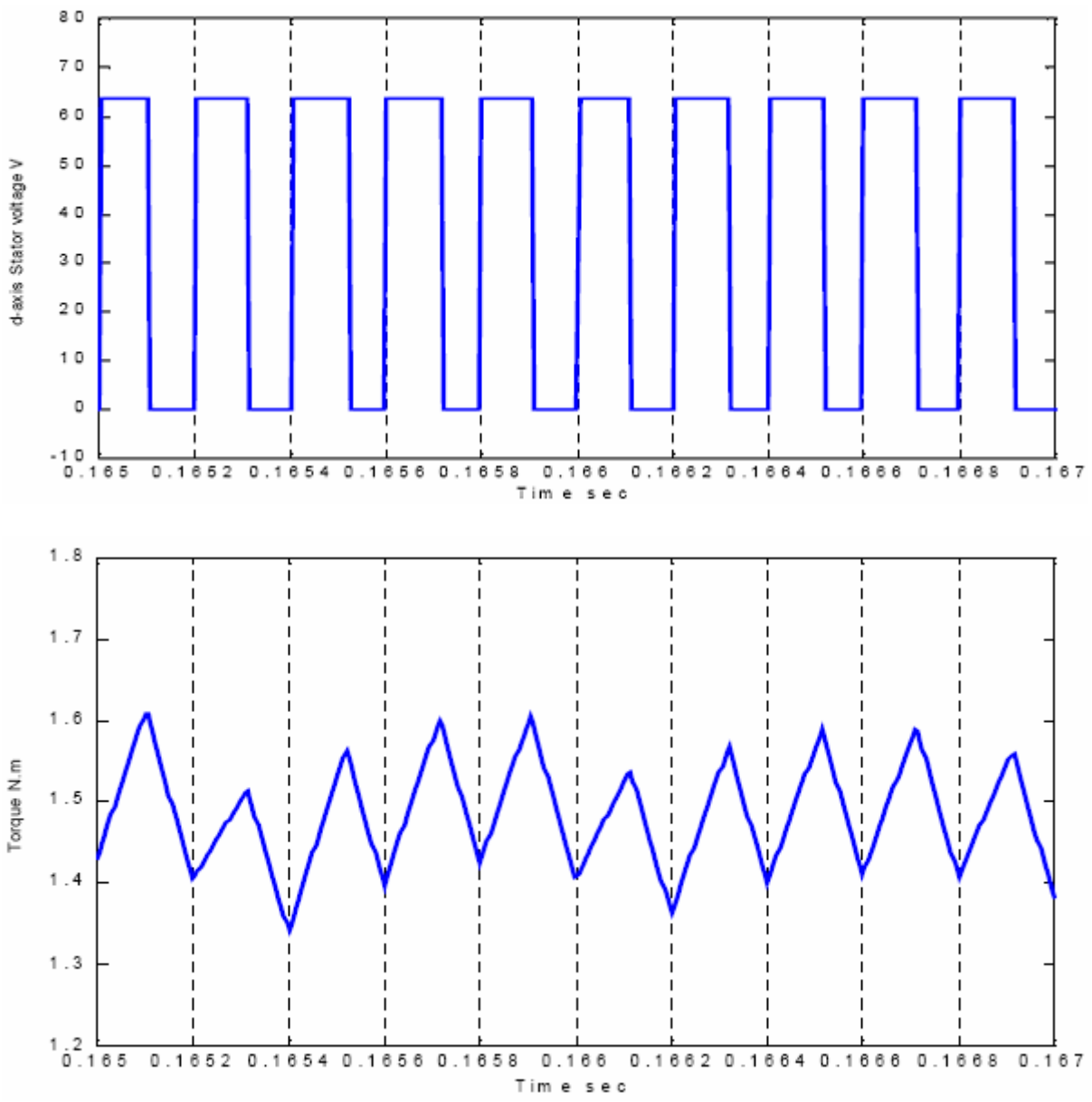

Fig 5.7 Voltage and torque switching in DTC with duty ratio fuzzy controller

Chapter 6

SIMULATION RESULTS

SIMULATION RESULTS

A MATLAB programme is developed to study the performance of the conventional DTC and DTC with duty ratio fuzzy controller for 4 pole Induction Motor torque control, and also a SIMULINK model is developed and simulated for the same and verified. Constant torque and flux commands of 1.5 Nm and 0.16Wb were used. The simulation was run at switching frequency of 5 kHz with a 110-V DC bus voltage. The parameters for the induction motor are

Rs	Rr	Lr	Ls	Lm
1.7Ω	4.3 Ω	0.084H	0.084H	0.082H

Table 6.1 Parameters of three phase induction motor

The induction motor was simulated using a state space model which is developed in chapter II. The SIMULINK model for DTC with duty ratio fuzzy controller is as shown in figure 6.1

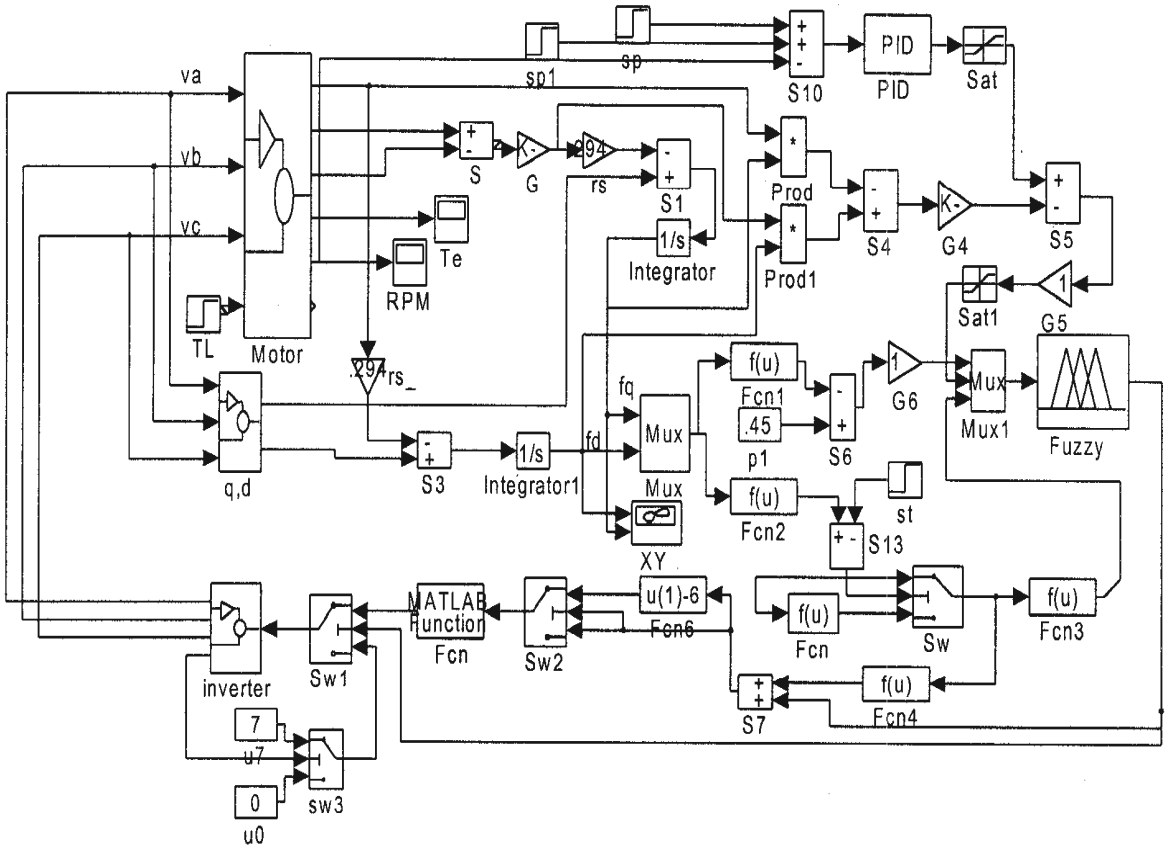

Fig 6.1 SIMULINK model for DTC with duty ratio fuzzy controller

Figs. 6.2 and 6.3 shows the torque response of the motor using conventional DTC and DTC with the duty ratio fuzzy control respectively for a step torque command of 1.5 Nm with the drive output updated at a rate of 5 kHz. The torque ripple is 0.6 Nm (approximately 1.8-1.2 Nm maximum and minimum values respectively) with the conventional DTC while with DTC with the duty ratio fuzzy control the ripple is reduced to 0.32 Nm (approximately 1.62-1.38 Nm maximum and minimum values respectively, neglecting the undershoot in the torque value at the beginning of each voltage sector)

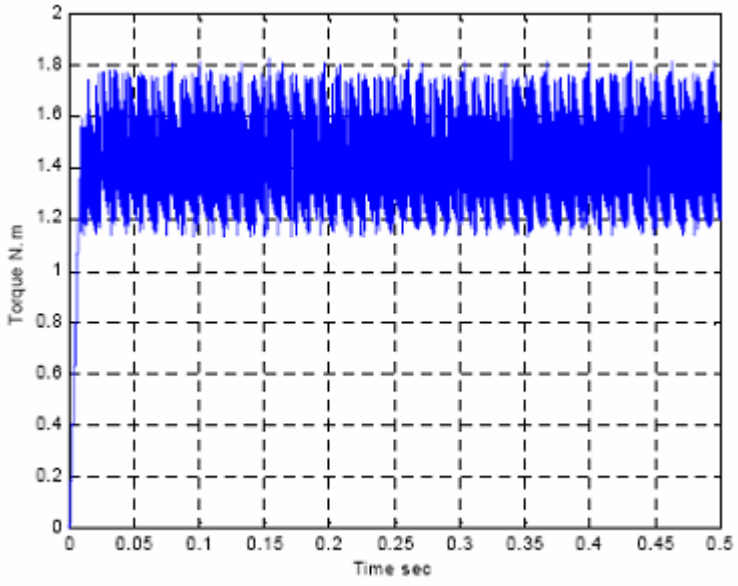

Fig 6.2 Electric torque of induction motor using conventional DTC

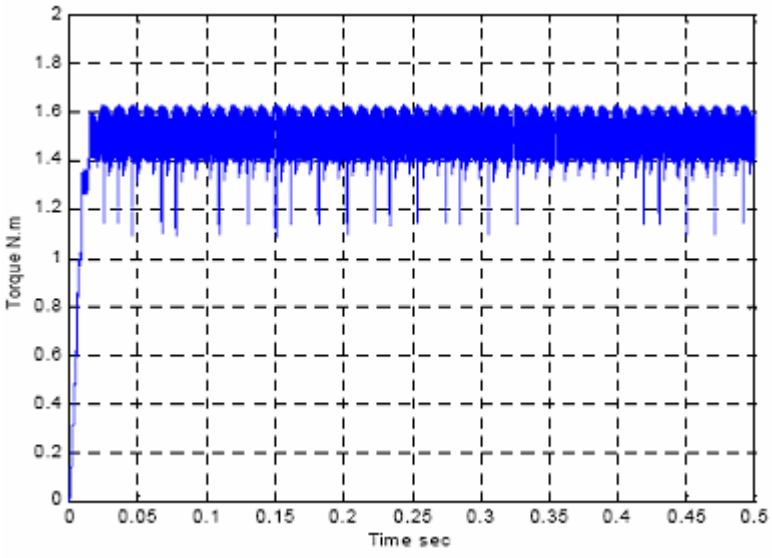

Fig 6.3 Electric torque of induction motor using DTC with duty ratio fuzzy controller

The waveforms of stator current for both conventional DTC and DTC with fuzzy duty ratio controller are shown in figures

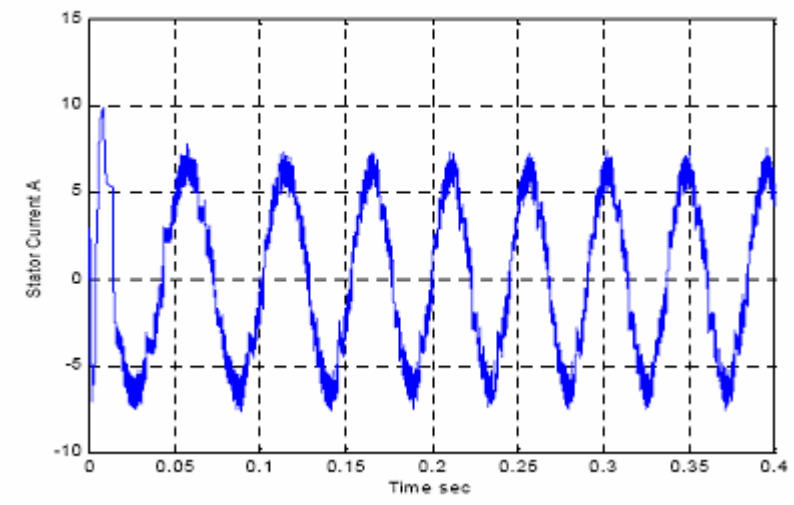

a) Using conventional DTC

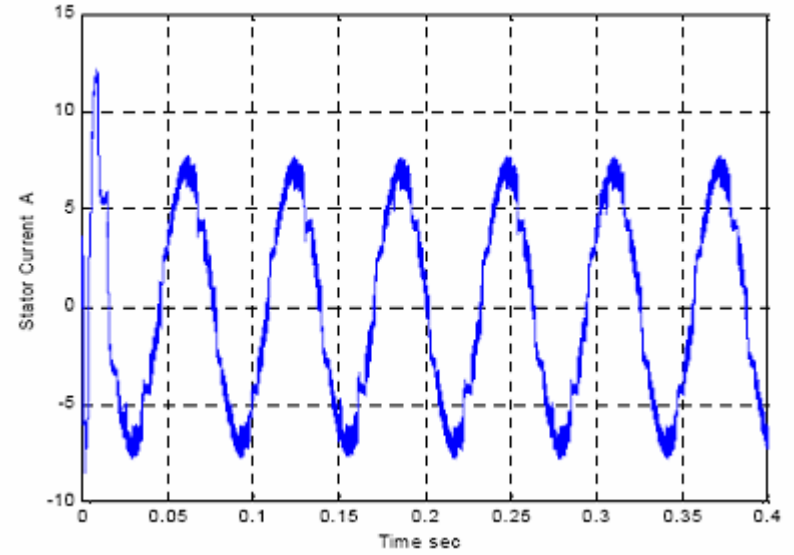

b) Using DTC with duty ratio fuzzy controller

Fig 6.4 Induction motor stator current waveforms

Fig 6.5 shows the stator flux vector locus of the motor using conventional DTC and DTC with the duty ratio fuzzy control, respectively with the controller output updated at a rate of 5 kHz. The duty ratio fuzzy control reduces the stator flux ripple,

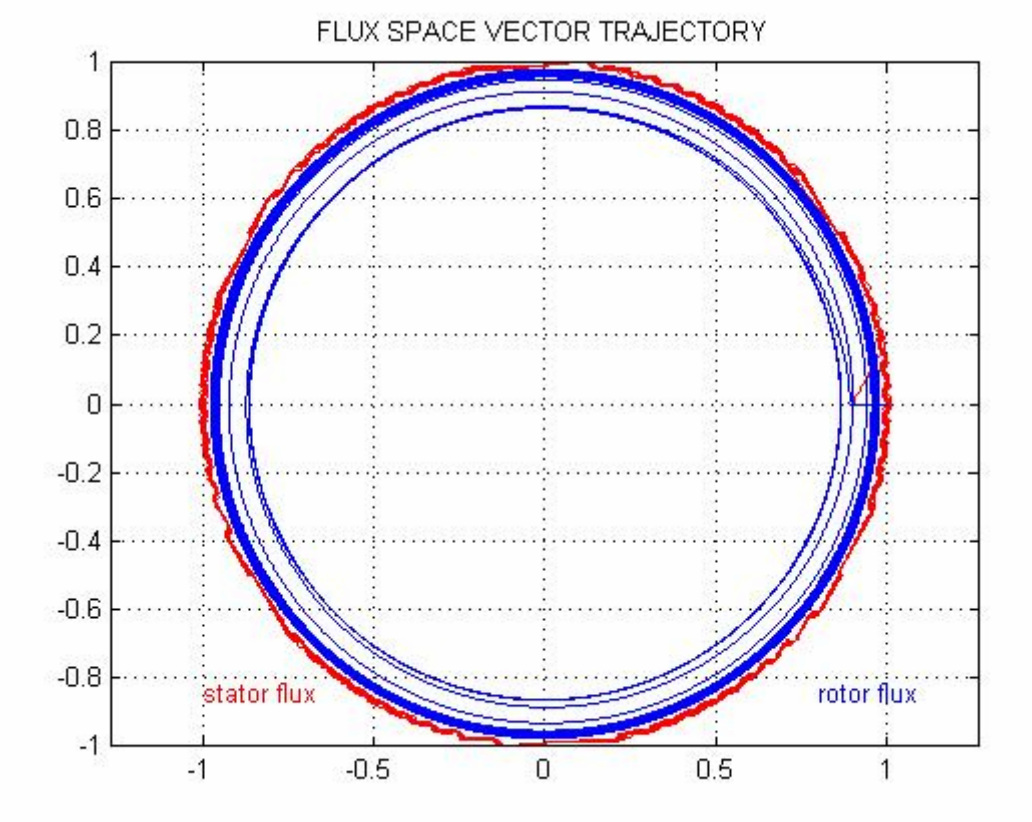

a) using conventional DTC

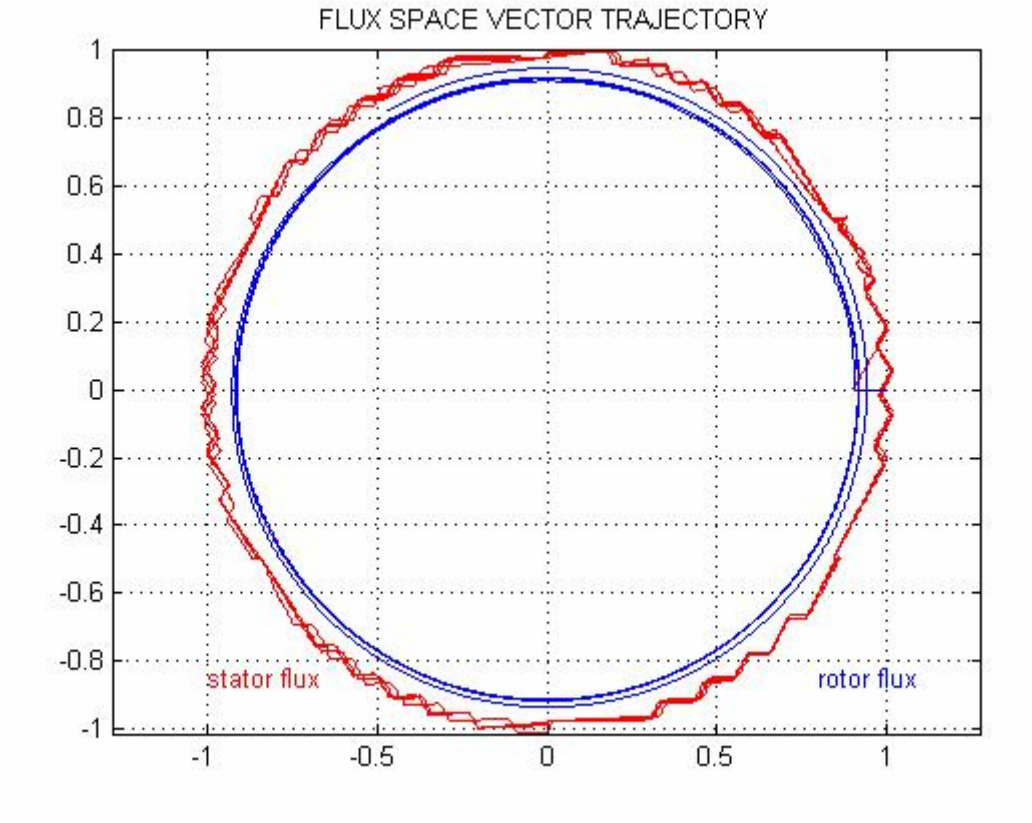

b) Using DTC with duty ratio fuzzy controller

Fig 6.5 stator and rotor flux phasor locus of induction motor

Chapter 7

Conclusions and future work

Conclusions

Future Work

CONCLUSIONS AND FUTURE WORK

7.1 CONCLUSIONS:

7.1.1 - Direct Torque Control.

Direct Torque Control is supposed to be one of the best controllers for driving any induction motor. Its main principles have been introduced and deeply explained. It is also demonstrated in this thesis that the method of DTC also allows the independent and decoupled control of motor torque and motor stator flux.

A SIMULINK/MATALB® model has been fully developed. From the results it is apparent that DTC strategy is simpler to implement than the flux vector control method because voltage modulators and co-ordinate transformations are not required. Although, it introduces some disadvantages, being the torque ripple one of the worst.

7.1.2 Direct torque control with duty ratio fuzzy controller:

After all the simulation work on conventional DTC done, this thesis is focused on introducing a modulation in the DTC. A Fuzzy Logic Controller is in charge of controlling this modulation between the selected active state and a null one. Therefore, it has been suggested and deeply described the Fuzzy Logic Controller, which together with the DTC will create the Fuzzy Logic DTC.

Finally, the theoretical claim that duty ratio control can reduce torque ripple in DTC induction motor drives was verified by simulation and experiment. The use of fuzzy logic control gave satisfactory results and reduces the computation burden by avoiding unnecessary complex mathematical modeling of the nonlinear systems. By using duty ratio control a specific motor performance can be achieved at a lower switching frequency compared to the conventional DTC, which in turn increases the efficiency of the drive by reducing losses due to currents and flux harmonics.

7.2 Future work:

All future work is summarized schematically in the following ideas:

- Developments of new fuzzy controllers to achieve better performance. This new fuzzy controller should, at least, take into account the following ideas:
    1. Develop a completely auto adaptive controller.
    2. The controller must be adaptive to any motor.
    3. Try to overcome the electrical noises, which appear in any power drive.

- Study the torque ripple reduction not only with fuzzy duty ratio controllers but also with multilevel converters..
- Sensor less Fuzzy logic DTC implementation, just sensing two currents and the DC voltage and by means of either Kalman filter techniques or observers.
- Study and apply different Fuzzy logic DTCs, not only to induction motors as it has been done in the present thesis, but also to any electrical motor.

REFERENCES:

[1] Takahashi, I. and Noguchi, T. "A new quick-response and high efficiency control Strategy of an induction motor." IEEE Transactions on Industry Applications, vol.22, no. 5, pp. 820-827, 1986.

[2] Novotny, D. W. and Lipo, T. A. “Vector Control and Dynamics of AC Drives.” Oxford University Press Inc, New York, 1996.

[3] Vas, P. " Sensor less Vector and Direct Torque Control". Oxford University Press 1998.

[4] Bose, B. K.; "Power Electronics and AC Drives". Prentice-Hall. 1986.

[5] Mohan, Undeland, Robbins. “Power Electronics". Wiley. Second edition. 1989.

[6] Ludtke, I.; Jayne M.G. “A comparative study of high performance speed control strategies for voltage sourced PWM inverter fed induction motor drives”, Seventh International Conference on electrical Machines and Drives, 11-13 September 1995, University of Durham, UK.

[7] Tamai, S., Sugimoto, H. and Yano, M. "Speed sensorless vector control of induction motor with model reference adaptive system." IEEE Industrial Applications Society Annual Meeting, Atlanta, pp.189-195, 1987.

[8] Schauder, C. "Adaptive speed identification for vector control of induction motors without rotational transducers." IEEE Transactions on Industrial Applications, vol.28, pp. 1054-1061, 1992.

[9] Doki, S., Sangwongwanich, S. and Okuma, S. "Implementation of speed sensorless field oriented vector control using adaptive sliding observer." IEEE-IECON, San Diego, pp. 453-458, 1992.

[10] Kawamura, A. and Hoft, R. "An analysis of induction motor for field oriented or vector control." IEEE Power Electronics Specialists Conference, Albuquerque, New Mexico, pp. 91-100, 1983.

[11] Kubota, H. and Matsuse, K. "Speed sensorless field oriented control of induction machines." IEEE IECON, Bologna, Italy, pp. 1611-1615, 1994.

[12] Mir, S. and Elbuluk, M. "Precision torque control in inverter fed induction machines using fuzzy logic". Conf. Rec. IEEE-PESC Annual Meeting, Atlanta, pp. 396-401, 1995.

[13] Depenbrock, M. "Direct self control (DSC) of inverter–fed induction machine." IEEE Transactions on Power Electronics, vol. 3, no. 4, pp. 420-429, 1988.

[14] Mir, S. and Elbuluk, M. "Precision torque control in inverter fed induction machines using fuzzy logic." Conf. Rec. IEEE-PESC Annual Meeting, Atlanta, pp. 396-401, 1995.

[15] Thomas, G., Halbetler, H. and Deepakraj, M. D. "Control strategies for direct torque control using discrete pulse modulation." IEEE Transactions on Industry Applications, vol. 27, pp. 893-901, 1991.

[16] Takahashi, I and Ohimori, Y. “High-Performance Direct Torque Control of an Induction Motor”, IEEE Trans. Industry Applications, Vol. 25, pages 257-264, March 1989.

[17] Perelmuter, V. "Three level inverters with direct torque control.” IEEE Proc. on Industry Applications, pp. 1368-1373, 2000.

[18] MATLAB Fuzzy logic toolbox user guide. The MathWorks, Inc, 1999.

[19] S. Mir, D. Zinger and M. Elbuluk, "Fuzzy controller for inverter-fed induction machine," *IEEE Trans. Ind. Appl.*, vol. 30, 1994, no. 1, pp. 78-84.

[20] Y.Xia W.Oghanna " Study on Fuzzy Control of Induction Machine With Direct Torque Control Approach " *,IEEE Catalog Number: 97TH8280- ISIE'97 - GuimarBes, Portugal*

[21] A.A.Pujol, “*Improvement in Direct Torque Control of Induction Motors”*, Doctoral Thesis de L’UPC, November 2000

[22] Hui-Hui Xia0, Shan Li, Pei-Lin Wan, Ming-Fu Zhao, "Study on Fuzzy Direct Torque Control System" *Proceedings of the Fourth International Conference on Machine Learning and Cybernetics, Beijing, 4-5 August 2002.*

[23] Wang, L. X. "Adaptive fuzzy systems and control: design and stability analysis." Englewood Cliffs, NJ. Prentice Hall, 1994.